

Real Elliptically Skewed Distributions and Their Application to Robust Cluster Analysis

Christian A. Schroth and Michael Muma, *Member, IEEE*

Abstract—This article proposes a new class of Real Elliptically Skewed (RESK) distributions and associated clustering algorithms that integrate robustness and skewness into a single unified cluster analysis framework. Non-symmetrically distributed and heavy-tailed data clusters have been reported in a variety of real-world applications. Robustness is essential because a few outlying observations can severely obscure the cluster structure. The RESK distributions are a generalization of the Real Elliptically Symmetric (RES) distributions. To estimate the cluster parameters and memberships, we derive an expectation maximization (EM) algorithm for arbitrary RESK distributions. Special attention is given to a new robust skew-Huber M-estimator, which is also the approximate maximum likelihood estimator (MLE) for the skew-Huber distribution, that belongs to the RESK class. Numerical experiments on simulated and real-world data confirm the usefulness of the proposed methods for skewed and heavy-tailed data sets.

Index Terms—robust cluster analysis, real elliptically skewed distributions, EM algorithm, heavy-tailed mixture models, multivariate RES distributions, M-estimator, robust data science, unsupervised learning, skew-Gaussian, skew-t, skew-Huber

I. INTRODUCTION

FINITE mixture models have been extensively used in cluster analysis to estimate the probability density function (pdf) of a given data set [1]–[5]. It is well-known that estimators that have been derived under a Gaussian data assumption are strongly affected by outliers, which frequently occur in real-world applications [6]–[8]. A popular remedy is to choose a heavy-tailed finite mixture model, such as, a member of the real elliptically symmetric (RES) family of distributions. The associated maximum-likelihood-estimators (MLE) can handle outliers and heavy-tailed noise. M-estimators provide further robustness, as they decouple the estimation from a specific distribution. The underlying idea is to replace the negative log-likelihood function by a robustness-inducing objective function [9]–[12].

While the RES distributions offer a high degree of flexibility in modeling different types of heavy-tailedness in the data distribution, they still depend on the assumption that the data is symmetrically distributed. However, in medical [13], [14], localization [15], [16] or financial [17] applications, it is often the case that the data is heavy-tailed *and* non-symmetrically distributed. The focus of this work, therefore, lies on mixture models that account for such cases. The proposed robust clustering algorithms are designed to provide reliable results, even if the data distribution is skewed, heavy-tailed, and if the data set contains outliers. A widely used

estimation algorithm for mixture models is the expectation maximization (EM) algorithm [1]. The standard EM algorithm is based on a Gaussian assumption [18], hence, it is not robust against outliers. Some efforts were made to robustify the EM by outlier detection and removal [19]–[22], assuming t-distributed/heavy-tailed data [23]–[25], using an additional component in a mixture model [26], [27], including contaminated Gaussian distributions [28] or robustifying the estimation of the cluster centers and covariances [29]. Recently, an EM algorithm has been derived that is applicable to any RES distribution [30]. An important member of the RES family, is the so-called Huber distribution, for which the popular Huber M-estimator is the MLE.

Multivariate skewed distributions include the skew-Gaussian distribution [31], [32], the skew-t distribution [33] and skew-Laplace distribution [34]. A summary of different skewed distributions can be found in [35], [36]. In contrast to RES distributions, there are multiple formulations for skewed distributions and, generally speaking, none of the specific formulations seems to be preferable over the others [37], [38]. In this work, we use the formulation introduced by [39] because it allows for deriving an EM algorithm with explicit solutions for the model parameters. This does not seem to be possible, for example, for the generalized multivariate skewed distributions introduced in [40], [41].

EM algorithms are available for a wide range of specific skewed distributions, e.g., for the skew-Gaussian [39], [42]–[47], the skew-t [45], [46], [48], [49], the skew power exponential [50] and the generalized hyperbolic [51]. Nevertheless to the best of our knowledge, a unified estimation framework for a broad class of skewed distributions has not yet been developed.

To fit a finite mixture model to a given data set, the EM algorithm requires the number of clusters to be known, or estimated. A popular strategy is to use model selection criteria, such as, the Bayesian Information Criterion (BIC) derived by Schwarz [52], [53]. Alternatively, a Bayesian cluster enumeration approach that selects the model that is maximum *a posteriori* most probable [54], [55] may be beneficial, because it accounts for the structure of the clustering problem in the penalty term.

Based on [39], [45]–[47], our main contribution is to propose a formulation for Real Elliptically Skewed (RESK) distributions and to derive an EM algorithm for such distributions. The RESK family of distributions is a generalization of the RES family of distributions, which are included within the RESK class by choosing an appropriate value for the skewness factor. For robustness purposes, our framework is then generalized to include asymmetric M-estimators, where

C. A. Schroth and M. Muma are with the Signal Processing Group at Technische Universität Darmstadt, Germany. mail: {schroth, muma}@spg.tu-darmstadt.de

Manuscript submitted, June 29, 2020.

special attention is given to a new skew-Huber's M-estimator. Numerical experiments demonstrate increased parameter estimation and cluster enumeration performance for skewed and heavy-tailed data.

The paper is organized as follows. Section II briefly revisits RES distributions and loss functions. Section III introduces the proposed RESK family of distributions with special attention given to the skew-Huber distribution. Section IV derives the proposed EM algorithm for RESK distributions and Section V briefly describes cluster enumeration for RESK distributions based on the Schwarz BIC. Simulations and real-world examples are provided and discussed in Section VI. Finally, conclusions are drawn and some possible future steps are mentioned in Section VII.

Notation: Normal-font letters (a, A) denote a scalar, bold lowercase (\mathbf{a}) a vector and bold uppercase (\mathbf{A}) a matrix; calligraphic letters (\mathcal{A}) denote a set, with the exception of \mathcal{L} , which is used for the likelihood function; \mathbb{R} is the set of real numbers and $\mathbb{R}^{r \times 1}$, $\mathbb{R}^{r \times r}$ the set of column vectors of size $r \times 1$ and matrices of size $r \times r$, respectively; \mathbf{A}^{-1} is the matrix inverse; \mathbf{A}^\top is the matrix transpose; $|a|$ is the absolute value of a scalar; $|\mathbf{A}|$ is the determinant of a matrix; \otimes represents the Kronecker product; $\text{vec}(\cdot)$ is the vectorization operator, \mathbf{D} is the duplication matrix and $\text{vech}(\cdot)$ is the vector half operator as defined in [56]. The vech operator takes a symmetric $r \times r$ matrix and stacks the lower/upper triangular half into a single vector of length $\frac{r}{2}(r+1)$.

II. RES DISTRIBUTIONS & LOSS FUNCTIONS

A. RES Distributions

Assuming that the observed data $\mathbf{x} \in \mathbb{R}^{r \times 1}$ follows a RES distribution with centroid $\boldsymbol{\mu} \in \mathbb{R}^{r \times 1}$ and positive definite symmetric scatter matrix $\mathbf{S} \in \mathbb{R}^{r \times r}$, the pdf of \mathbf{x} is given by

$$f(\mathbf{x}|\boldsymbol{\mu}, \mathbf{S}, g) = |\mathbf{S}|^{-\frac{1}{2}} g(t), \quad (1)$$

where $t = (\mathbf{x} - \boldsymbol{\mu})^\top \mathbf{S}^{-1} (\mathbf{x} - \boldsymbol{\mu})$ is the squared Mahalanobis distance, see [7, p. 109] and [41]. The function g , often referred to as the density generator, is defined by

$$g(t) = \frac{\Gamma(\frac{r}{2})}{\pi^{r/2}} \left(\int_0^\infty u^{r/2-1} h(u; r) du \right)^{-1} h(t; r), \quad (2)$$

where $h(t; r)$ is a function for which

$$\int_0^\infty u^{r/2-1} h(u; r) du < \infty \quad (3)$$

holds. Note that $h(t; r)$ can be a function of multiple parameters, not only of r .

B. Loss Functions

Assuming an observation of N independent and identically distributed (iid) random variables denoted by $\mathcal{X} = \{\mathbf{x}_1, \dots, \mathbf{x}_N\}$, the associated likelihood function is given by

$$\mathcal{L}(\boldsymbol{\mu}, \mathbf{S}|\mathcal{X}) = \prod_{n=1}^N \left| \mathbf{S}^{-1} \right|^{\frac{1}{2}} g(t_n) \quad (4)$$

with $t_n = (\mathbf{x}_n - \boldsymbol{\mu})^\top \mathbf{S}^{-1} (\mathbf{x}_n - \boldsymbol{\mu})$. The MLE minimizes the negative log-likelihood function

$$\begin{aligned} -\ln(\mathcal{L}(\boldsymbol{\mu}, \mathbf{S}|\mathcal{X})) &= -\ln \left(\prod_{n=1}^N \left| \mathbf{S}^{-1} \right|^{\frac{1}{2}} g(t_n) \right) \\ &= \sum_{n=1}^N -\ln(g(t_n)) - \frac{N}{2} \ln \left(\left| \mathbf{S}^{-1} \right| \right) \\ &= \sum_{n=1}^N \rho_{\text{ML}}(t_n) + \frac{N}{2} \ln(|\mathbf{S}|) \end{aligned} \quad (5)$$

where the ML loss function [7, p. 109] is defined as

$$\rho_{\text{ML}}(t_n) = -\ln(g(t_n)). \quad (6)$$

The corresponding first and second derivatives are denoted, respectively, by

$$\psi_{\text{ML}}(t_n) = \frac{\partial \rho_{\text{ML}}(t_n)}{\partial t_n}, \quad \eta_{\text{ML}}(t_n) = \frac{\partial^2 \psi_{\text{ML}}(t_n)}{\partial t_n^2}. \quad (7)$$

The key idea of M-estimation [9] is to replace the ML loss function $\rho_{\text{ML}}(t_n)$ in Eq. (6) with a more general loss function $\rho(t_n)$. The aim of robust M-estimators is not necessarily to be optimal for a single specific distribution, but to provide near-optimal performance within a neighborhood of distributions including heavy-tailed distributions. The weight function $\psi(t_n)$ can be designed according to desired robustness properties. For example, the very popular Huber weight function down weights outlying data points while giving full weight to points with a small Mahalanobis distance. Interestingly, Huber's estimator is not only a popular M-estimator, but it also has been shown to be the MLE for a specific RES distribution. An overview of some exemplary loss functions and their derivatives can be found in Tables I and II. Since the Gaussian and t distribution are well-known they are not further discussed, but for the Huber distribution a brief discussion is provided in Section III-C.

III. RESK DISTRIBUTIONS

A. Definition of RESK Distributions

This section proposes the class of RESK distributions as a generalization of RES distributions to allow for skewness. Well-known skewed distributions, such as, the skew-Gaussian and the skew-t [14], [41], [45]–[47] distribution are included as special cases. The aim is to provide a unified framework to derive robust clustering algorithms for skewed data. Based on the RESK distributions, the user is given a large flexibility in designing algorithms that fit to skewed and heavy-tailed data. This is because the proposed formulation allows for the derivation of an explicit solution for the EM algorithm for arbitrary RESK distributions. As an example, a new clustering algorithm by skewing Huber's distribution is derived.

Assuming that the observed data $\mathbf{x} \in \mathbb{R}^{r \times 1}$ follows a RESK distribution, let $\boldsymbol{\xi} \in \mathbb{R}^{r \times 1}$ be the 'centroid', $\boldsymbol{\lambda} \in \mathbb{R}^{r \times 1}$ the skewness factor and let $\mathbf{S} \in \mathbb{R}^{r \times r}$ be the positive definite symmetric scatter matrix. Then, it is possible to define the RESK distribution as a RES distribution multiplied with its univariate cdf

$$f_s(\mathbf{x}|\boldsymbol{\xi}, \mathbf{S}, \boldsymbol{\lambda}, g) = 2 |\boldsymbol{\Omega}|^{-\frac{1}{2}} g(\underline{t}) F(\kappa(\underline{t})) \quad (8)$$

with the skewed scatter matrix

$$\mathbf{\Omega} = \mathbf{S} + \boldsymbol{\lambda}\boldsymbol{\lambda}^\top, \quad (9)$$

the skewed squared Mahalanobis distance

$$\underline{t} = (\mathbf{x} - \boldsymbol{\xi})^\top \mathbf{\Omega}^{-1} (\mathbf{x} - \boldsymbol{\xi}) \quad (10)$$

and

$$\kappa(\underline{t}) = \frac{\eta}{\tau} \sqrt{2\psi(\underline{t})} \quad (11)$$

with $\psi(t)$ from Table I. The normalization factor '2' in Eq. (8) arises naturally from the multiplication with the cdf of a RES distribution, because every cdf of a RES distribution has a mean value of 1/2. This result can be easily verified by taking the symmetry of the RES distributions into account. Hence, the same result is obtained by evaluating $F(0) = 1/2$. To simplify the notation, the argument of $\kappa(\underline{t})$ is dropped and the following scalar variables are introduced:

$$\eta = \frac{\boldsymbol{\lambda}^\top \mathbf{S}^{-1} (\mathbf{x} - \boldsymbol{\xi})}{1 + \boldsymbol{\lambda}^\top \mathbf{S}^{-1} \boldsymbol{\lambda}}, \quad \tau^2 = \frac{1}{1 + \boldsymbol{\lambda}^\top \mathbf{S}^{-1} \boldsymbol{\lambda}} \quad (12)$$

Figure 1a illustrates the flexibility in modeling skewed data by plotting the univariate skew-Gaussian distribution for different values of the skewness parameter λ . In the multivariate case, the skewness vector $\boldsymbol{\lambda}$ allows for different amounts of skewness in every dimension. Figure 1b shows the influence of the centroid $\boldsymbol{\xi}$, which for the univariate case simply shifts the distribution to the left or right. In the multivariate case, $\boldsymbol{\xi}$ shifts independently the distribution in each dimension. While the figure illustrates these parameters for the skew-Gaussian distribution, their meaning is identical for other RESK distributions.

We next briefly revisit some known special cases of RESK distributions before introducing the skew-Huber distribution. All required functions are summarized in Tables I and II.

B. Examples of Known Existing RESK Distributions

1) *RES Distributions*: The RESK distribution has the property that, for $\boldsymbol{\lambda} = \mathbf{0}$, it is equal to a RES distribution as defined in Eq. (1), because $\eta = 0$, $\tau = 1$ and $\kappa(\underline{t}) = 0$, which leads to $F(0) = 1/2$. Also, one can find that $\boldsymbol{\xi} = \boldsymbol{\mu}$, hence the RESK distribution is a generalization of the RES distribution. This can be also observed in Figure 1a. By comparing the black dashed curve with the red curve, it becomes clear that, for $\lambda = 0$, the skew-Gaussian is equal to the Gaussian distribution.

2) *Skew-Gaussian Distribution*: The pdf is defined by

$$\phi_s(\mathbf{x}|\boldsymbol{\xi}, \mathbf{S}, \boldsymbol{\lambda}) = 2\phi(\mathbf{x}|\boldsymbol{\xi}, \mathbf{\Omega})\Phi\left(\frac{\eta}{\tau}\right) \quad (13)$$

with $\phi(\mathbf{x}|\boldsymbol{\mu}, \boldsymbol{\Sigma})$ being the multivariate pdf and $\Phi(x)$ being the univariate cdf of the Gaussian distribution.

3) *Skew-t Distribution*: The pdf is defined by

$$t_s(\mathbf{x}|\boldsymbol{\xi}, \mathbf{S}, \boldsymbol{\lambda}, \nu) = 2t(\mathbf{x}|\boldsymbol{\xi}, \mathbf{\Omega}, \nu)T_{\nu+r}(\kappa(\underline{t})), \quad (14)$$

where $t(\mathbf{x}|\boldsymbol{\mu}, \boldsymbol{\Psi}, \nu)$ is the multivariate pdf and $T_\nu(x)$ is the univariate cdf of a t distribution with associated degree of freedom parameter ν . During our work with the skew-t distribution we came across some inconsistencies regarding the definition of \underline{t} and $\frac{\eta}{\tau}$ of the skew-t distribution between [46] and [47]. These inconsistencies are corrected here and the correct expressions are given in Eqs. (10) and (12).

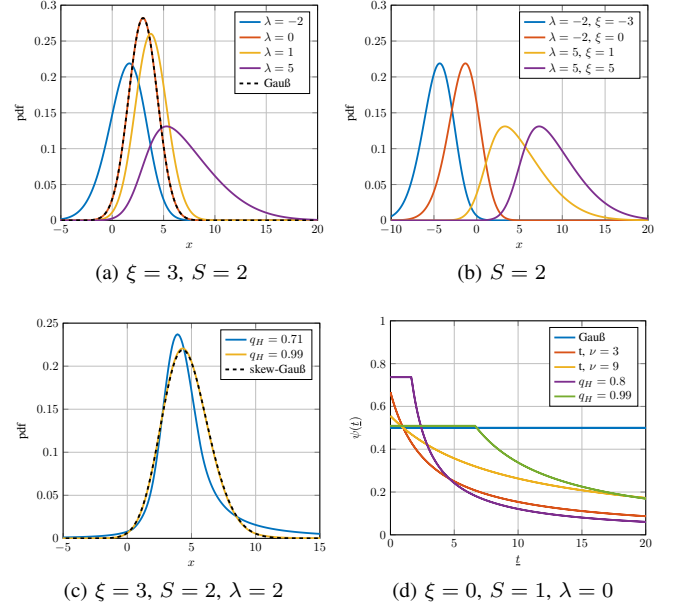


Fig. 1. The upper left figure shows some exemplary skew-Gaussian pdfs for different values of λ . For $\lambda = 0$, the skew-Gaussian distribution is equal to the Gaussian distribution. In the upper right figure, the influence of $\boldsymbol{\xi}$ is examined, as it shifts the pdf to the left or right. In the lower left figure, the skew-Huber distribution is shown for different values of q_H from Eq. (27). For $q_H \rightarrow 1$ the skew-Huber distribution becomes more and more equal to the skew-Gaussian distribution, while smaller values of q_H result in heavier tails. A similar behavior can be observed in the lower right figure, that shows the weight function $\psi(\underline{t})$ for different distributions and different values of q_H .

C. Proposed Skew-Huber Distribution

Based on the definition in Eq. (8), the skew-Huber distribution can now be introduced as

$$h_s(\mathbf{x}|\boldsymbol{\xi}, \mathbf{S}, \boldsymbol{\lambda}, c) = 2h(\mathbf{x}|\boldsymbol{\xi}, \mathbf{\Omega}, c)H_c(\kappa(\underline{t})) \quad (15)$$

with the multivariate Huber pdf from Eq. (22) and the univariate Huber cdf from Eq. (24), which are derived in the following.

1) *Multivariate pdf of Huber Distribution*: Huber's M-estimator can be seen as the ML estimator for a specific RES distribution (the Huber distribution) [7, p. 115], [57, p. 8]. It is defined by

$$h(t; r, c) = \exp\left(-\frac{1}{2}\rho_H(t; c)\right) \quad (16)$$

with some tuning constant $c \geq 0$ and

$$\rho_H(t; c) = \begin{cases} \frac{t}{b} & , t \leq c^2 \\ \frac{c^2}{b} \left(\ln\left(\frac{t}{c^2}\right) + 1 \right) & , t > c^2 \end{cases}. \quad (17)$$

To obtain Fisher consistency

$$b = F_{\chi_{r+2}}^2(c^2) + \frac{c^2}{r} \left(1 - F_{\chi_r}^2(c^2)\right), \quad (18)$$

where $F_{\chi_r}^2(\cdot)$ is the Chi-square cumulative distribution function with degree of freedom r . For $h(t; r, c)$ to be a valid pdf

the normalization factor, according to [41], has to be calculated as

$$\begin{aligned} & \int_0^\infty u^{r/2-1} h(u; r, c) du \\ &= \int_0^{c^2} u^{r/2-1} e^{-\frac{u}{2b}} du + \int_{c^2}^\infty u^{r/2-1} \left(\frac{eu}{c^2}\right)^{-\frac{c^2}{2b}} du \\ &= (2b)^{r/2} \left(\Gamma\left(\frac{r}{2}\right) - \Gamma\left(\frac{r}{2}, \frac{c^2}{2b}\right) \right) + \frac{2bc^r \exp\left(-\frac{c^2}{2b}\right)}{c^2 - br}, \end{aligned} \quad (19)$$

with the gamma function $\Gamma(\cdot)$, the upper incomplete gamma function $\Gamma(\cdot, \cdot)$ and Euler's number e . The density generator, see Eq. (1), of a Huber distribution now follows as

$$g(t) = \begin{cases} A_H \exp\left(-\frac{t}{2b}\right) & , t \leq c^2 \\ A_H \left(\frac{et}{c^2}\right)^{-\frac{c^2}{2b}} & , t > c^2 \end{cases}, \quad (20)$$

with

$$A_H = \frac{\Gamma\left(\frac{r}{2}\right)}{\pi^{r/2}} \left((2b)^{\frac{r}{2}} \left(\Gamma\left(\frac{r}{2}\right) - \Gamma\left(\frac{r}{2}, \frac{c^2}{2b}\right) \right) + \frac{2bc^r e^{-\frac{c^2}{2b}}}{c^2 - br} \right)^{-1}. \quad (21)$$

Then, the multivariate Huber pdf is obtained as

$$h(\mathbf{x}|\boldsymbol{\mu}, \mathbf{S}, c) = \begin{cases} |\mathbf{S}|^{-\frac{1}{2}} A_H \exp\left(-\frac{t}{2b}\right) & , t \leq c^2 \\ |\mathbf{S}|^{-\frac{1}{2}} A_H \left(\frac{et}{c^2}\right)^{-\frac{c^2}{2b}} & , t > c^2 \end{cases} \quad (22)$$

2) *Univariate cdf of Huber Distribution:* We start with the univariate pdf

$$h(x|\mu, s, c) = \begin{cases} \frac{A_H}{s} e^{-\frac{(x-\mu)^2}{2bs^2}} & , \left| \frac{x-\mu}{s} \right| \leq c \\ \frac{A_H}{s} \left(\frac{e(x-\mu)^2}{c^2 s^2} \right)^{-\frac{c^2}{2b}} & , \left| \frac{x-\mu}{s} \right| > c \end{cases} \quad (23)$$

and integrate it. This leads to

$$H_c(z) = \begin{cases} \frac{A_H b z}{b - c^2} \left(\frac{ez^2}{c^2} \right)^{-\frac{c^2}{2b}} & , z < -c \\ \frac{-A_H b c}{b - c^2} e^{-\frac{c^2}{2b}} & , |z| \leq c \\ + A_H \sqrt{\frac{\pi b}{2}} \left(\operatorname{erf}\left(\frac{z}{\sqrt{2b}}\right) + \operatorname{erf}\left(\frac{c}{\sqrt{2b}}\right) \right) & , |z| \leq c \\ \frac{-A_H b c}{b - c^2} e^{-\frac{c^2}{2b}} + A_H \sqrt{2\pi b} \operatorname{erf}\left(\frac{c}{\sqrt{2b}}\right) & , z > c \\ + \frac{A_H b}{b - c^2} \left(\frac{e}{c^2} \right)^{-\frac{c^2}{2b}} \left(z \left(z^2 \right)^{-\frac{c^2}{2b}} - c^{1-\frac{c^2}{b}} \right) & , z > c \end{cases} \quad (24)$$

with $z = \frac{x-\mu}{s}$ and the integrals

$$\begin{aligned} & \int_{-\infty}^z A_H \left(\frac{eu^2}{c^2} \right)^{-\frac{c^2}{2b}} du \\ &= A_H \left(\frac{e}{c^2} \right)^{-\frac{c^2}{2b}} \frac{b}{b - c^2} \left[u \left(u^2 \right)^{-\frac{c^2}{2b}} \right]_{-\infty}^z \\ &= A_H \left(\frac{e}{c^2} \right)^{-\frac{c^2}{2b}} \frac{b}{b - c^2} \left(z \left(z^2 \right)^{-\frac{c^2}{2b}} - \lim_{u \rightarrow -\infty} u \left(u^2 \right)^{-\frac{c^2}{2b}} \right) \\ &= A_H \left(\frac{e}{c^2} \right)^{-\frac{c^2}{2b}} \frac{b}{b - c^2} z \left(z^2 \right)^{-\frac{c^2}{2b}} \end{aligned} \quad (25)$$

with the constraint $\frac{c^2}{2b} > 1$ and

$$\begin{aligned} & \int_{-c}^z A_H \exp\left(-\frac{u^2}{2b}\right) du \\ &= A_H \sqrt{\frac{\pi b}{2}} \left(\operatorname{erf}\left(\frac{z}{\sqrt{2b}}\right) + \operatorname{erf}\left(\frac{c}{\sqrt{2b}}\right) \right). \end{aligned} \quad (26)$$

When deriving estimators based on the Huber distribution, [7, p. 116] suggest to choose c^2 as the q_H th upper quantile of a χ_r^2 distribution

$$c^2 = F_{\chi_r^2}^{-1}(q_H), \quad 0 < q_H < 1. \quad (27)$$

The value of q_H is chosen to trade-off efficiency under a Gaussian model and robustness against outliers. We can proceed similarly for the skew-Huber, but from $\frac{c^2}{2b} > 1$ in Eq. (25), we have the constraint that $q_H > 0.703$. In Figure 1c, the skew-Huber distribution is plotted over different values of q_H from Eq. (27). For lower values of q_H , probability mass is shifted to the tails of the distribution. As $q_H \rightarrow 1$ and $c \rightarrow \infty$ the skew-Huber becomes equal to the skew-Gaussian distribution. Additionally, in Figure 1d the influence of the weight function $\psi(t)$ is shown. Similarly, as $q_H \rightarrow 1$ and $c \rightarrow \infty$ the weight function becomes equal to the Gaussian weight function.

IV. PROPOSED EXPECTATION MAXIMIZATION ALGORITHM FOR A MIXTURE OF RESK DISTRIBUTIONS

In this section, we derive an EM algorithm to estimate the RESK mixture model parameters and the cluster memberships of the data vectors \mathbf{x}_n by alternating the E- and M-steps until convergence. The proposed approach is summarized in Algorithm 1, where we provide a unified EM clustering framework that is beneficial for skewed and heavy-tailed data sets. The user simply chooses a RESK density generator $g(t)$ and determines the associated weight function $\psi(t)$. We have implemented some specific variants of the EM algorithm, for example the skew-Huber, based on the values from Tables I and II. However, the framework is not limited to these cases, and therefore it is very flexible in modeling different data distributions.

The parameter vector, for each cluster $m = 1, \dots, l$, is defined as $\boldsymbol{\theta}_m = [\boldsymbol{\xi}_m^\top, \boldsymbol{\lambda}_m^\top, \operatorname{vech}(\mathbf{S}_m)^\top]^\top \in \mathbb{R}^{q \times 1}$, where

TABLE I
OVERVIEW OF $g(t_n)$, $\rho(t_n)$ AND $\psi(t_n)$ FUNCTIONS

	$g(t_n)$	$\rho(t_n)$	$\psi(t_n)$
Gaussian	$(2\pi)^{-\frac{r}{2}} \exp(-\frac{1}{2}t_n)$	$\frac{1}{2}t_n + \frac{r}{2} \ln(2\pi)$	$\frac{1}{2}$
t	$\frac{\Gamma((\nu+r)/2)}{\Gamma(\nu/2)(\pi\nu)^{r/2}} \left(1 + \frac{t_n}{\nu}\right)^{-(\nu+r)/2}$	$-\ln\left(\frac{\Gamma((\nu+r)/2)}{\Gamma(\nu/2)(\pi\nu)^{r/2}}\right) + \frac{\nu+r}{2} \ln\left(1 + \frac{t_n}{\nu}\right)$	$\frac{1}{2} \cdot \frac{\nu+r}{\nu+t_n}$
Huber	$\begin{cases} A_H \exp\left(-\frac{t_n}{2b}\right) & , t_n \leq c^2 \\ A_H \left(\frac{t_n}{c^2}\right)^{-\frac{c^2}{2b}} \exp\left(-\frac{c^2}{2b}\right) & , t_n > c^2 \end{cases}$	$\begin{cases} -\ln(A_H) + \frac{t_n}{2b} & , t_n \leq c^2 \\ -\ln(A_H) + \frac{c^2}{2b} \left(\ln\left(\frac{t_n}{c^2}\right) + 1\right) & , t_n > c^2 \end{cases}$	$\begin{cases} \frac{1}{2b} & , t_n \leq c^2 \\ \frac{c^2}{2bt_n} & , t_n > c^2 \end{cases}$

TABLE II
OVERVIEW OF $\eta(t_n)$ AND $\Psi(x)$ FUNCTIONS

	$\eta(t_n)$	$\Psi(x)$
Gaussian	0	$-\frac{\phi(x 0,1)}{\Phi(x)}$ *
t	$-\frac{1}{2} \cdot \frac{\nu+r}{(\nu+t_n)^2}$	$-\frac{t(x 0,1,\nu+r)}{T_{\nu+r}(x)}$
Huber	$\begin{cases} 0 & , t_n \leq c^2 \\ -\frac{c^2}{2bt_n^2} & , t_n > c^2 \end{cases}$	$-\frac{h(x 0,1,c)}{H_c(x)}$

* The calculation of $\Psi(x)$ can be numerically unstable, due to the fact that $\Phi(x)$ tends to zero for $x < -37$. An approximation for these values can be found in [46, p. 29].

l is the number of clusters and $q = \frac{r}{2}(r+5)$ is the number of parameters per cluster. Because \mathbf{S}_m is symmetric, it has only $\frac{r}{2}(r+1)$ unique elements. Therefore, $\text{vech}(\mathbf{S}_m)$ has to be used in the estimation step [58, p. 367]. Accordingly, we derive an EM algorithm for RESK distributions in the following.

Based on Equation (8), the mixture of l RESK distributions is formulated as

$$p(\mathbf{x}|\Phi_l) = \sum_{m=1}^l \gamma_m f_s(\mathbf{x}|\boldsymbol{\theta}_m) \quad (28)$$

and the incomplete data log-likelihood follows as

$$\begin{aligned} \ln(\mathcal{L}(\Phi_l|\mathcal{X})) &= \ln(p(\mathcal{X}|\Phi_l)) \\ &= \sum_{n=1}^N \ln\left(\sum_{m=1}^l \gamma_m f_s(\mathbf{x}|\boldsymbol{\theta}_m)\right) \end{aligned} \quad (29)$$

with γ_m being the mixing coefficient and $\Phi_l = [\boldsymbol{\gamma}_l, \boldsymbol{\Theta}_l^\top]$ with $\boldsymbol{\gamma}_l = [\gamma_1, \dots, \gamma_l]^\top$ and $\boldsymbol{\Theta}_l = [\boldsymbol{\theta}_1, \dots, \boldsymbol{\theta}_l] \in \mathbb{R}^{q \times l}$.

Following the derivation of the EM algorithm from [18], a latent binary variable $\mathbf{z} = [z_1, \dots, z_l]^\top$ is introduced, which has a single component equal to 1 and all other components equal to 0. The conditional distribution of \mathbf{x} given \mathbf{z} , becomes

$$p(\mathbf{x}|\mathbf{z}, \boldsymbol{\Theta}_l) = \prod_{m=1}^l f_s(\mathbf{x}|\boldsymbol{\theta}_m)^{z_m}, \quad (30)$$

where the prior of the latent variables is given by

$$p(\mathbf{z}|\boldsymbol{\gamma}_l) = \prod_{m=1}^l \gamma_m^{z_m} \quad (31)$$

and the joint distribution equals

$$p(\mathbf{x}, \mathbf{z}|\Phi_l) = \prod_{m=1}^l (\gamma_m f_s(\mathbf{x}|\boldsymbol{\theta}_m))^{z_m}. \quad (32)$$

Now, the complete data log-likelihood, with \mathcal{X} and $\mathcal{Z} = \{\mathbf{z}_1, \dots, \mathbf{z}_N\}$, is formulated as

$$\begin{aligned} \ln(p(\mathcal{X}, \mathcal{Z}|\Phi_l)) &= \ln\left(\prod_{n=1}^N \prod_{m=1}^l (\gamma_m f_s(\mathbf{x}_n|\boldsymbol{\theta}_m))^{z_{nm}}\right) \\ &= \sum_{n=1}^N \sum_{m=1}^l z_{nm} (\ln(\gamma_m) + \ln(f_s(\mathbf{x}_n|\boldsymbol{\theta}_m))), \end{aligned} \quad (33)$$

where z_{nm} denotes the m th element of \mathbf{z}_n . For the E-step the expected value of the complete data log-likelihood with respect to the latent variables is calculated as

$$\begin{aligned} E_{\mathcal{Z}}[\ln(p(\mathcal{X}, \mathcal{Z}|\Phi_l))] &= Q(\Phi_l) \\ &= \sum_{n=1}^N \sum_{m=1}^l v_{nm} (\ln(\gamma_m) + \ln(f_s(\mathbf{x}_n|\boldsymbol{\theta}_m))) \end{aligned} \quad (34)$$

with

$$\begin{aligned} v_{nm} &= E[z_{nm}] = \sum_{z_{nm}} z_{nm} p(z_{nm}|\mathbf{x}_n, \gamma_m, \boldsymbol{\theta}_m) \\ &= \sum_{z_{nm}} \frac{z_{nm} p(z_{nm}|\gamma_m) p(\mathbf{x}_n|z_{nm}, \boldsymbol{\theta}_m)}{p(\mathbf{x}_n|\gamma_m, \boldsymbol{\theta}_m)} \\ &= \sum_{z_{nm}} \frac{z_{nm} (\gamma_m f_s(\mathbf{x}_n|\boldsymbol{\theta}_m))^{z_{nm}}}{\sum_{z_{nm}} (\gamma_m f_s(\mathbf{x}_n|\boldsymbol{\theta}_m))^{z_{nm}}} \\ &= \frac{\sum_{j=1}^l \gamma_j f_s(\mathbf{x}_n|\boldsymbol{\theta}_j)}{\sum_{j=1}^l \gamma_j f_s(\mathbf{x}_n|\boldsymbol{\theta}_j)}. \end{aligned} \quad (35)$$

The calculation of the ML estimates when using the EM algorithm requires fixed values for the variable v_{nm} and

additionally for $e_{0,nm}$, $e_{1,nm}$ and $e_{2,nm}$ from Eqs. (53), (54) and (64). In the E-step of the EM algorithm v_{nm} is fixed with respect to θ_m by calculating the expected value of z_{nm} . A latent variable approach would be also favorable for $e_{0,nm}$, $e_{1,nm}$ and $e_{2,nm}$, but it turns out, that for general RESK distributions this is not feasible. Hence, $e_{0,nm}$, $e_{1,nm}$ and $e_{2,nm}$ are approximated by the estimated values $\hat{\theta}_m$ of the previous iteration of the EM algorithm into Eqs. (53), (54) and (64) which yields the approximations $\tilde{e}_{0,nm}$, $\tilde{e}_{1,nm}$ and $\tilde{e}_{2,nm}$. If the approximations hold exactly, which is the case e.g. for the skew-Gaussian distribution, the ML estimate is obtained. Otherwise an approximate ML estimate is obtained. In the context of M-estimation, where the primary aim is trading off near-optimality at a nominal distribution for robustness over a family of distributions [7], [9], such an approximation is well motivated and of high practical value. Based on the approximations, the expected value of the complete data log-likelihood, is maximized, which results in the following estimates for the M-step:

$$\hat{\xi}_m = \frac{\sum_{n=1}^N v_{nm} (\tilde{e}_{0,nm} \mathbf{x}_n - \tilde{e}_{1,nm} \boldsymbol{\lambda}_m)}{\sum_{n=1}^N v_{nm} \tilde{e}_{0,nm}}, \quad (36)$$

$$\hat{\lambda}_m = \frac{\sum_{n=1}^N v_{nm} \tilde{e}_{1,nm} \tilde{\mathbf{x}}_n}{\sum_{n=1}^N v_{nm} \tilde{e}_{2,nm}} \quad (37)$$

with $\tilde{\mathbf{x}}_n = \mathbf{x}_n - \xi_m$,

$$\hat{S}_m = \left[\sum_{n=1}^N v_{nm} (\tilde{e}_{0,nm} \tilde{\mathbf{x}}_n \tilde{\mathbf{x}}_n^\top - \tilde{e}_{1,nm} \tilde{\mathbf{x}}_n \boldsymbol{\lambda}_m^\top - \tilde{e}_{1,nm} \boldsymbol{\lambda}_m \tilde{\mathbf{x}}_n^\top + \tilde{e}_{2,nm} \boldsymbol{\lambda}_m \boldsymbol{\lambda}_m^\top) \right] / \sum_{n=1}^N v_{nm}, \quad (38)$$

and

$$\hat{\gamma}_m = \frac{1}{N} \sum_{n=1}^N v_{nm}. \quad (39)$$

A detailed derivation of the M-step is given in Appendix A.

V. CLUSTER ENUMERATION

This section gives a brief overview of the Schwarz BIC [52], [53], which we use to estimate the number of clusters. There exist alternative criteria, e.g. [30], [59], [60], but in this paper the focus does not lie on cluster enumeration. Hence, only the log-likelihood function is adapted to RESK distributions and the Schwarz BIC is applied, i.e.

$$\text{BIC}_o(M_l) = \sum_{m=1}^l \ln(\mathcal{L}(\hat{\theta}_m | \mathcal{X}_m)) - \frac{ql}{2} \ln(N) \quad (40)$$

with M_l being a candidate model with $l \in \{L_{\min}, \dots, L_{\max}\}$ clusters. The true number of clusters K is assumed to lie within $L_{\min} \leq K \leq L_{\max}$. For the RES case, the log-likelihood function is

$$\ln(\mathcal{L}(\hat{\theta}_m | \mathcal{X}_m)) = - \sum_{\mathbf{x}_n \in \mathcal{X}_m} \rho(\hat{t}_{nm}) + N_m \ln\left(\frac{N_m}{N}\right) - \frac{N_m}{2} \ln(|\hat{S}_m|). \quad (41)$$

Algorithm 1: EM algorithm for RESK distribution

Input: \mathcal{X} , i_{\max} , l , $g(t)$, $\psi(t)$

Output: $\hat{\xi}_m$, \hat{S}_m , $\hat{\lambda}_m$, $\hat{\gamma}_m$

for $m = 1, \dots, l$ **do**

Initialize $\hat{\xi}_m^{(0)}$, e.g. with K-means or K-medoids

Initialize $\hat{\lambda}_m^{(0)} = \mathbf{1}$

$$\hat{S}_m^{(0)} = \frac{1}{N_m} \sum_{\mathbf{x}_n \in \mathcal{X}_m} (\mathbf{x}_n - \hat{\xi}_m^{(0)}) (\mathbf{x}_n - \hat{\xi}_m^{(0)})^\top$$

$$\hat{\gamma}_m^{(0)} = \frac{N_m}{N}$$

for $i = 1, \dots, i_{\max}$ **do**

E-step:

for $m = 1, \dots, l$ **do**

for $n = 1, \dots, N$ **do**

Calculate $\hat{v}_{nm}^{(i)}$, $\tilde{e}_{0,nm}^{(i)}$, $\tilde{e}_{1,nm}^{(i)}$ and $\tilde{e}_{2,nm}^{(i)}$ with Eqs. (35), (53), (54) and (64) using the estimates from the previous iteration

M-Step:

for $m = 1, \dots, l$ **do**

$$\hat{\xi}_m^{(i)} = \frac{\sum_{n=1}^N \hat{v}_{nm}^{(i)} (\tilde{e}_{0,nm}^{(i)} \mathbf{x}_n - \tilde{e}_{1,nm}^{(i)} \hat{\lambda}_m^{(i-1)})}{\sum_{n=1}^N \hat{v}_{nm}^{(i)} \tilde{e}_{0,nm}^{(i)}}$$

$$\hat{\lambda}_m^{(i)} = \frac{\sum_{n=1}^N \hat{v}_{nm}^{(i)} \tilde{e}_{1,nm}^{(i)} (\mathbf{x}_n - \hat{\xi}_m^{(i)})}{\sum_{n=1}^N \hat{v}_{nm}^{(i)} \tilde{e}_{2,nm}^{(i)}}$$

$$\hat{S}_m^{(i)} = \left[\sum_{n=1}^N \hat{v}_{nm}^{(i)} [\tilde{e}_{0,nm}^{(i)} \hat{\mathbf{x}}_n^{(i)} (\hat{\mathbf{x}}_n^{(i)})^\top - \tilde{e}_{1,nm}^{(i)} \hat{\mathbf{x}}_n^{(i)} (\hat{\lambda}_m^{(i)})^\top - \tilde{e}_{1,nm}^{(i)} \hat{\lambda}_m^{(i)} (\hat{\mathbf{x}}_n^{(i)})^\top + \tilde{e}_{2,nm}^{(i)} \hat{\lambda}_m^{(i)} (\hat{\lambda}_m^{(i)})^\top] \right] / \sum_{n=1}^N \hat{v}_{nm}^{(i)}$$

with $\hat{\mathbf{x}}_n^{(i)} = \mathbf{x}_n - \hat{\xi}_m^{(i)}$

$$\hat{\gamma}_m^{(i)} = \frac{1}{N} \sum_{n=1}^N \hat{v}_{nm}^{(i)}$$

Calculate log-likelihood:

$$\ln(\mathcal{L}(\hat{\Phi}_l^{(i)} | \mathcal{X})) = \sum_{n=1}^N \ln\left(\sum_{m=1}^l \hat{\gamma}_m^{(i)} 2 \left|\hat{\Omega}_m^{(i)}\right|^{-\frac{1}{2}} \times g\left(\frac{\hat{t}_{nm}^{(i)}}{\hat{t}_{nm}^{(i)}}\right) F\left(\hat{k}_{nm}^{(i)}\right)\right)$$

if $|\ln(\mathcal{L}(\hat{\Phi}_l^{(i)} | \mathcal{X})) - \ln(\mathcal{L}(\hat{\Phi}_l^{(i-1)} | \mathcal{X}))| < \delta$
then

break loop

For the RESK case, the log-likelihood function is derived as

$$\begin{aligned} \ln(\mathcal{L}(\hat{\boldsymbol{\theta}}_m | \mathcal{X}_m)) &= - \sum_{\mathbf{x}_n \in \mathcal{X}_m} \rho(\hat{t}_{nm}) + N_m \ln \left(\frac{N_m}{N} \right) + N_m \ln(2) \\ &\quad - \frac{N_m}{2} \ln \left(\left| \hat{\boldsymbol{\Omega}}_m \right| \right) + \sum_{\mathbf{x}_n \in \mathcal{X}_m} \ln(F(\hat{\kappa}_{nm})). \end{aligned} \quad (42)$$

The number of clusters is estimated by evaluating

$$\hat{K} = \arg \max_{l=L_{\min}, \dots, L_{\max}} \text{BIC}_o(M_l). \quad (43)$$

VI. EXPERIMENTAL RESULTS

This section reports on our numerical experiments to evaluate the proposed EM algorithms based on RESK distributions in terms of (i) their parameter estimation and clustering performance for skewed and heavy-tailed mixture models; (ii) their robustness against outliers; (iii) their convergence speed in terms of the number of required iterations; and (iv) their ability to model real-world data. We compare the newly proposed skew-Huber estimator to other known estimators, such as the skew-Gaussian, skew-t [46], and the classic Gaussian, t- and Huber estimators. An implementation of the proposed EM algorithm and the conducted simulations is available at: <https://github.com/schrchr/Real-Elliptically-Skewed-Distributions>.

A. Dataset 1

The first data set is comprised of $K = 3$ skew-Gaussian distributed clusters. It is generated with the algorithm from [46, p. 23], and $\mathbf{x}_k \sim \mathcal{N}_s(\boldsymbol{\xi}_k, \boldsymbol{\Sigma}_k, \boldsymbol{\lambda}_k)$, $k = 1, 2, 3$. The cluster centroids are chosen as $\boldsymbol{\xi}_1 = [2, 3.5]^\top$, $\boldsymbol{\xi}_2 = [6, 2]^\top$ and $\boldsymbol{\xi}_3 = [10, 3]^\top$, the skewness factors are $\boldsymbol{\lambda}_1 = [10, 4]^\top$, $\boldsymbol{\lambda}_2 = [1, -2]^\top$ and $\boldsymbol{\lambda}_3 = [2, 1]^\top$ and the covariance matrices are given by

$$\boldsymbol{\Sigma}_1 = \begin{bmatrix} 0.2 & 0.1 \\ 0.1 & 0.75 \end{bmatrix}, \boldsymbol{\Sigma}_2 = \begin{bmatrix} 0.5 & 0.25 \\ 0.25 & 0.5 \end{bmatrix}, \boldsymbol{\Sigma}_3 = \begin{bmatrix} 1 & 0.5 \\ 0.5 & 1 \end{bmatrix}.$$

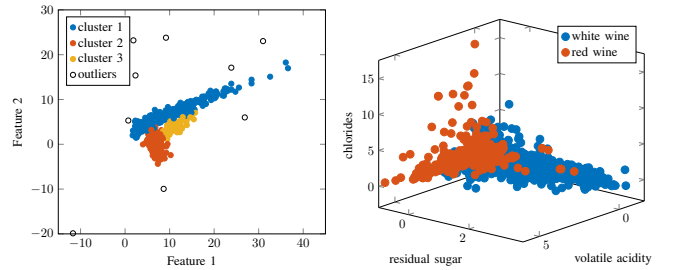
The number of data points per cluster is specified as $N_1 = 5 \times N_K$, $N_2 = 4 \times N_K$ and $N_3 = 1 \times N_K$. An exemplary realization is given in Figure 2a.

B. Dataset 2

The second data set comprised of $K = 2$ skew-t distributed clusters is generated with the algorithm from [46, p. 23], and $\mathbf{x}_k \sim \mathcal{T}_s(\boldsymbol{\xi}_k, \mathbf{S}_k, \boldsymbol{\lambda}_k, \nu_k)$, $k = 1, 2, 3$. The cluster centroids are chosen as $\boldsymbol{\xi}_1 = [2, 3.5]^\top$ and $\boldsymbol{\xi}_2 = [7, -2]^\top$, the skewness factors are $\boldsymbol{\lambda}_1 = [4, 3]^\top$ and $\boldsymbol{\lambda}_2 = [1, -2]^\top$, the degrees of freedom are set to $\nu_1 = \nu_2 = 3$ and the covariance matrices are given by

$$\mathbf{S}_1 = \begin{bmatrix} 0.2 & 0.1 \\ 0.1 & 0.75 \end{bmatrix}, \mathbf{S}_2 = \begin{bmatrix} 0.5 & 0.25 \\ 0.25 & 0.5 \end{bmatrix}.$$

The number of data points per cluster is specified as $N_1 = N_2 = N_K$.



(a) Simulated data with $\epsilon = 2\%$ replacement outliers. (b) First three features of the wine data.

Fig. 2. Exemplary realizations of the simulated data set and the wine set.

C. Outlier Generation

To study robustness against outliers, an ϵ -contamination model is used, where ϵ denotes the percentage of randomly replaced data points. To make the clustering problem well-defined, it is assumed that the outliers do not form a cluster. Therefore, a uniform distribution is chosen as the outlier generating distribution because it produces isolated data points that are placed with equal probability on a sufficiently large area compared to the clustered data. For Dataset 1 and Dataset 2, the outliers are uniformly distributed in the range of $[-15, 45]$, $[-20, 30]$ in x, y-dimension.

D. Choice of Tuning Parameters

Based on [7, p. 121], for Huber's and skew-Huber's estimator, a value of $q_H = 0.8$ is chosen for all simulations, which leads to $c = 1.282$. For all t and skew-t distributions, $\nu = 3$ is selected for the degree of freedom. Both are common choices in M-estimation to trade-off robustness against outliers and efficiency for Gaussian data. To evaluate the choice of $\nu = 3$, we also report on an oracle version, where the degree of freedom is selected from the set $\nu = \{1, 2, 3, 4, 5, 7, 9\}$ so that it provides the optimal performance.

E. Performance Measures

1) *Kullback-Leibler Divergence*: To evaluate the parameter estimation performance of the proposed method, we use the Kullback-Leibler (KL) divergence, which measures the difference between two pdfs [61, p. 34]. It is defined as

$$D_{KL}(p||q) = \sum_{i=1}^N p(x_i) \ln \left(\frac{p(x_i)}{q(x_i)} \right) \quad (44)$$

with $p(x_i)$ representing the pdf that generates the outlier-free data and $q(x_i)$ representing the pdf estimated by the EM algorithm. Even if there are outliers in the data, the aim of robust methods is to provide information about $p(x_i)$. Therefore, the KL divergence between $p(x_i)$ and $q(x_i)$ is computed.

2) *Confusion Matrix*: To evaluate the correctness in labeling the non-outlying data points, the confusion matrix for these points is reported.

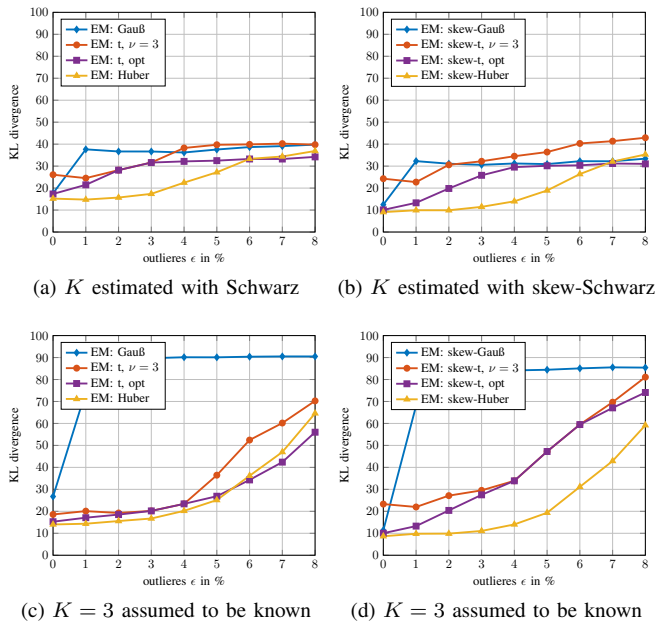


Fig. 3. Kullback–Leibler divergences between estimated and true pdfs for $N_K = 50$, over different amounts of outliers. A lower KL divergence value indicates better performance. The data is generated as an epsilon contamination mixture consisting of a skew-Gaussian for the clustered data and a uniform distribution for the outliers.

3) *Sensitivity Curve*: The sensitivity curve (also known as empirical influence function [7]) shows the effect of a single outlier as a function of its position in the feature space. The concept of looking at single outliers is related to infinitesimal robustness, or qualitative robustness, as measured by the influence function. A robust method is expected to provide a nearly optimal performance and is not largely influenced by a single outlier, irrespective of the value that the outlier takes. In our experiments, the sensitivity curves are calculated as follows. One randomly chosen sample is replaced with an outlier from the range $[-15, 45]$, $[-20, 30]$ in x, y -dimension. For each point of a grid of outlier values, the proposed EM algorithm is executed. The resulting estimated pdf is then compared with the true (outlier-free) generating pdf by calculating the KL divergence, which is averaged over 200 Monte Carlo iterations with $N_K = 50$.

4) *Breakdown Behavior*: Showing robustness against a single outlier is not sufficient in cluster analysis, where we may have positive a fraction of data points that do not follow the cluster structure of the remaining data points. This is several experiments with varying amounts of outliers are conducted. To analyze robustness against a fraction of outliers, data is generated from a mixture model with a nominal distribution (e.g. the Gaussian or the t) and a contaminating (outlier generating) distribution. The level of contamination is increased until all methods break down.

F. Results Based on Dataset 1: Robustness, Parameter Estimation and Clustering Accuracy

Figure 3 shows the KL divergences over different amounts of outlier contamination, averaged over 500 Monte Carlo

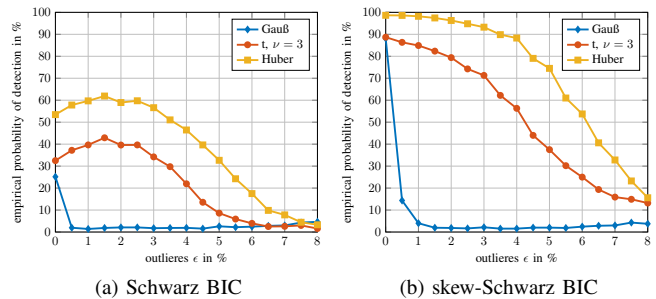


Fig. 4. Empirical probability of detection for the correct number of clusters over different amount of outliers, for $N_K = 50$ samples per cluster. The data is generated as an epsilon contamination mixture consisting of a skew-Gaussian for the clustered data and a uniform distribution for the outliers.

iterations. In the first row, the number of clusters is estimated with the Schwarz BIC from Eq. (40) and in the second row the true number of clusters is assumed to be known. By comparing the first column (RES ϵ model) with the second column (RESK model), it becomes clear that, for this simulation, the proposed skew-Huber model performs better than all other RES and RESK models. This is the case, because of Huber’s weight function $\psi(t_n)$ gives full weight to the data points with a squared distance smaller than c^2 while heavily down-weighting the outliers. One can also note that the skew- t with $\nu = 3$ is outperformed in all cases, and even the oracle method skew- t , opt is outperformed for almost all cases when K is assumed to be known. Until approximately 3% of outliers, the KL divergences for the true and estimated number of clusters are almost constant and similar, because in this range the Schwarz BIC has a very high empirical probability to detect the correct number of clusters, as shown in Figure 4b. When using RES distributions, such a high empirical probability of detection cannot be reached, see Figure 4a. As the amount of outliers increases and the performance of the Schwarz BIC starts to deteriorate, the KL divergence remains lower than for the case with the true number of clusters. This can be explained by the degree of freedom of opening up an additional cluster for the outliers, which leads to a deceptive better data fit, that is actually overfitting.

In Figure 5, six exemplary sensitivity curves are shown. The number of clusters is estimated with the Schwarz/skew-Schwarz BIC. As desired for a robust estimator, for this example, the skew-Huber estimator has the lowest KL divergence. It is almost not influenced by the position of the outlier, as indicated by the almost constant KL divergence over the grid. For the Gauß and skew-Gauß estimators, the performance quickly deteriorates as soon as the outlier is positioned outside the clusters. The other robust estimators, i.e. the t , skew- t and Huber show a stable but inferior performance compared to the skew-Huber estimator.

Tables III and IV show the confusion matrices with 0% and 2% of outliers. In the 0% case, all methods have a very high probability of assigning the data points to the correct cluster, with the best result for both Huber (RES and RESK) estimators. For 2% of outlier contamination, both Gaussian estimators break down, whereas the t and Huber

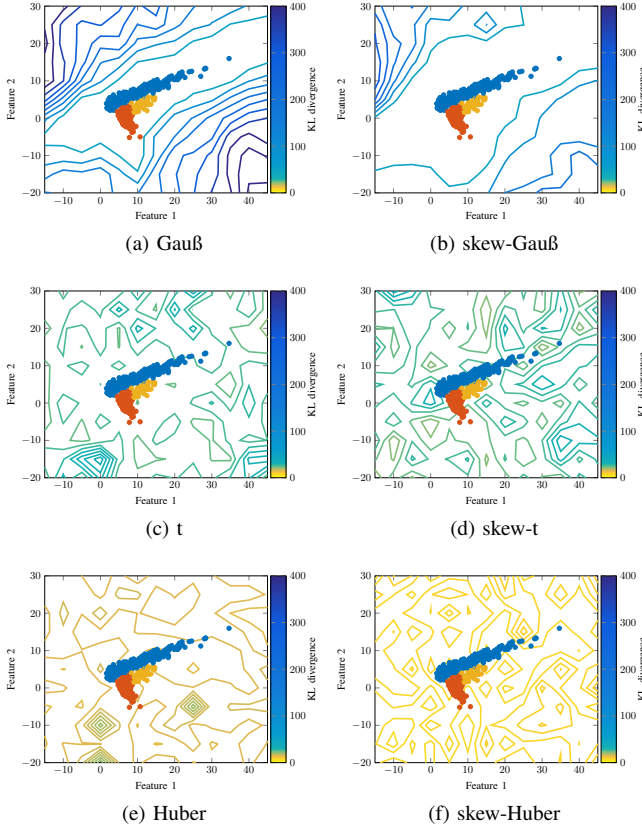


Fig. 5. Sensitivity curves for $N_K = 50$ that show six exemplary results for the KL divergence, while estimating K with the Schwarz/skew-Schwarz BIC, as a function of the single replacement outlier position. A lower KL divergence value indicates better performance. The clusters are generated from skew-Gaussian distributions and one randomly chosen sample is replaced with an outlier from the range $[-15, 45]$, $[-20, 30]$ in x , y -dimension.

based estimators are able to maintain the high performance from the 0% case, again, with the best result for the skew-Huber distribution based estimator.

G. Results Based on Dataset 2: Assessment of Bias and Convergence Speed

In this section, we examine the bias behavior and convergence speed based on Dataset 2. Because this data follows a skew-t distribution with $\nu = 3$, the skew-t, $\nu = 3$ is the MLE for $\epsilon = 0\%$ outliers. In Figure 6, we show the KL divergence over different amounts of outliers. As expected, the best performance can be observed for the skew-t estimator, closely followed by the skew-Huber estimator. As it can be seen from Figure 6b, the KL divergence nearly approaches zero for $\epsilon = 0\%$, which indicates, in combination with the low variance, that the bias of the algorithms is very small.

To assess the convergence speed of the EM algorithm, the average number of EM iterations is plotted in Figure 7. Two main observations can be made. Firstly, the RESK-based EM algorithm takes much longer to converge than the RES algorithm and, additionally, it has a much more varying stopping time. The anomaly of the skew-Gaussian based EM stopping faster for larger amount of outliers, can be probably

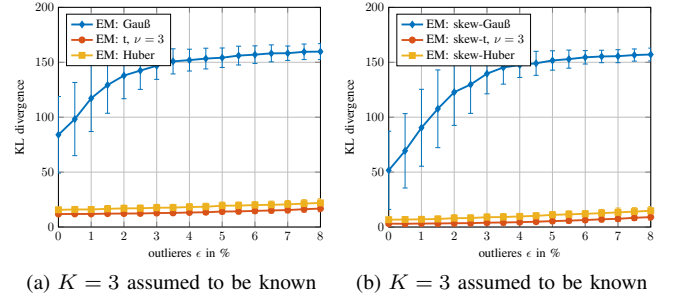


Fig. 6. Kullback-Leibler divergences between estimated and true pdfs for $N_K = 200$, over different amounts of outliers. A lower KL divergence value indicates better performance. The data is generated as an epsilon contamination mixture consisting of a skew-t with $\nu = 3$ for the clustered data and a uniform distribution for the outliers.

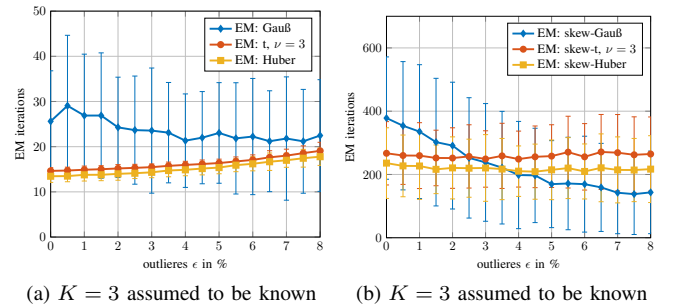


Fig. 7. EM iterations for $N_K = 200$, over different amounts of outliers. Less iterations indicate a better performance. The data is generated as an epsilon contamination mixture consisting of a skew-t with $\nu = 3$ for the clustered data and a uniform distribution for the outliers.

explained by the fact, that the algorithm completely breaks down and stops prematurely at a local optimum.

Lastly, to further investigate the bias behavior and convergence speed, the results of the EM algorithms are shown for different amounts of samples per cluster. No outliers are included in this case. As shown in Figure 8, the larger the amount of samples per cluster, the better the estimation of the true pdf and the lower the variance in the estimation. For a very large number of samples per cluster, the estimated and true pdf are almost identical. This confirms, for the given example, that the approximate ML estimate is near-optimal if the nominal model that is used in the EM algorithm and the data generating model match exactly. For the the RESK algorithms, the convergence speed of the EM algorithms increases for larger sample sizes, as shown in Figure 9.

H. Real Data Simulations

1) *Wine Data*: The wine quality data set from the UCI Machine Learning Repository (<https://archive.ics.uci.edu/ml/datasets/wine+quality>), is composed of 12 different attributes. To distinguish between red and white wine samples, we chose four attributes: volatile acidity, residual sugar, chlorides and total sulfur dioxide, from the data set. The first three attributes are visualized in Figure 2b. The number of clusters, i.e. $K = 2$ is assumed to be known and, to increase the difficulty, $\epsilon = 3\%$ of uniformly distributed replacement outliers are added in every dimension. From Table V, it is observed that the

TABLE III
CONFUSION MATRICES FOR SIMULATED DATA WITH $\epsilon = 0\%$

$\epsilon = 0\%$	Gauß			t			Huber			skew-Gauß			skew-t			skew-Huber			
	1	2	3	1	2	3	1	2	3	1	2	3	1	2	3	1	2	3	
true	1	87.2	1.5	11.3	95.6	2.6	1.8	95.4	1.9	2.7	94.9	1	4.1	93	1.5	5.5	97.4	1.4	1.2
	2	0.1	98.8	1.1	0	99.8	0.2	0	99.7	0.3	0.1	98.9	1	0	99.8	0.2	0	99.9	0.1
	3	3.2	1.1	95.7	3.7	2	94.3	3	1.9	95.1	1.9	1.3	96.8	3.1	4.6	92.3	2.1	3.5	94.4
\emptyset	93.9			96.5			96.7			96.9			95.1			97.2			

TABLE IV
CONFUSION MATRICES FOR SIMULATED DATA WITH $\epsilon = 2\%$

$\epsilon = 2\%$	Gauß			t			Huber			skew-Gauß			skew-t			skew-Huber			
	1	2	3	1	2	3	1	2	3	1	2	3	1	2	3	1	2	3	
true	1	96	2.3	1.7	94.9	2.8	2.3	94.2	1.9	3.9	98.1	1.2	0.7	89	1.7	9.3	96.4	1.4	2.2
	2	1.1	98.5	0.4	0	99.8	0.2	0.1	99.6	0.3	1.9	97.7	0.4	0.1	99.7	0.2	0	99.8	0.2
	3	83.3	3.8	12.9	4.1	2	93.9	3.7	1.9	94.4	76.9	11.5	11.6	4.5	5	90.5	2.4	3.4	94.2
\emptyset	69.1			96.1			96			69.1			93.1			96.8			

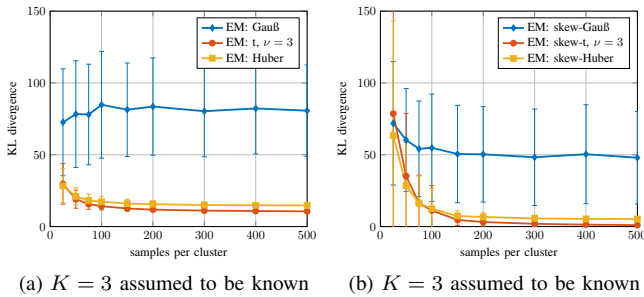


Fig. 8. Kullback–Leibler divergences between estimated and true pdfs, over different samples per cluster. A lower KL divergence value indicates better performance. The data is generated as a skew-t with $\nu = 3$ for the clustered data without any outlier contamination.

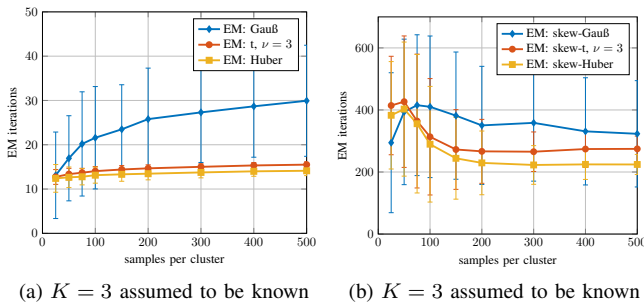


Fig. 9. EM iterations for $\epsilon = 0\%$, over different samples per cluster. Less iterations indicate a better performance. The data is generated as a skew-t with $\nu = 3$ for the clustered data without any outlier contamination.

modeling of skewness increases the probability of assigning a data point to the correct cluster. Again, the skew-Huber shows the best results.

2) *Crabs Data*: The crab data set was first used by [62] and can be downloaded at <https://doi.org/10.24097/wolfram.70344>. data. It is composed of five different length measurements on *Leptograpsus* crabs, of which all five were used to distinguish between blue/orange and male/female crabs. The number of clusters $K = 4$ is assumed to be known and no additional

outliers are added. Table VI and VII show, that the modeling of skewness, again, increases the overall performance. For this data set, the skew-t distribution based estimator showed best overall performance.

VII. CONCLUSION

We have presented a finite mixture model based on the proposed family of RESK distributions which is capable of integrating robustness and skewness into a single framework. Special attention was given to a newly proposed skew-Huber distribution, which has the attractive property that resulting estimators give maximal weight to data points with a distance smaller than a chosen threshold value while heavily down weighting outliers. The down weighting is asymmetric by taking skewness of the distribution into account. For the proposed family of RESK distributions, we derived an EM algorithm to estimate the cluster parameters and memberships. The performance was evaluated numerically in terms of parameter estimation and clustering performance for skewed and heavy-tailed mixture models, robustness against outliers, and convergence speed in terms of the number of required EM iterations. The proposed methods demonstrated promising performance on all simulated and real-world examples. This showcases their usefulness in simultaneously addressing skewness, outliers and heavy tailed data. The provided framework, therefore, could be useful in a variety of cluster analysis applications where the data may be skewed and heavy-tailed. Future work may consider deriving new robust cluster enumeration criteria and further robust M-estimators to cluster skewed data with outliers. New asymmetric M-estimators can be designed by varying the density generator within the class of RESK distributions according to the user’s preference in terms of weighting the data points. Future work may also include deriving a stochastic representation for the skew-Huber distribution or other M-estimators. Based on this stochastic representation, the corresponding approximate ML estimator could be replaced by the exact ML estimator.

TABLE V
CONFUSION MATRICES FOR THE WINE DATA SET.

$\epsilon = 3\%$		Gauß		t		Huber		skew-Gauß		skew-t		skew-Huber	
		1	2	1	2	1	2	1	2	1	2	1	2
true	1	97.8	2.2	87.1	12.9	67	33	97.8	2.2	93.6	6.4	93.7	6.3
	2	94.8	5.2	18	82	5.6	94.4	94.8	5.2	11.5	88.5	2.8	97.2
\emptyset		51.5		84.5		80.7		51.5		90.9		95.5	

TABLE VI
CONFUSION MATRICES FOR THE CRAB DATA SET.

		Gauß				t				Huber				
		1	2	3	4	1	2	3	4	1	2	3	4	
blue	male	1	33.7	14.9	25.5	25.9	90	10	0	0	38.2	18.5	26.2	17.1
	female	2	30	23.7	34.3	12	76.9	23.1	0	0	7	72.4	10.4	10.2
orange	male	3	26	11.2	38.8	24	0	10	40	50	19.9	10.4	40.8	28.9
	female	4	40.4	5.2	16.4	38	0	5.5	34.5	60	37.6	7.8	17.1	37.5
\emptyset		33.5				53.3				47.2				

TABLE VII
CONFUSION MATRICES FOR THE CRAB DATA SET.

		skew-Gauß				skew-t				skew-Huber				
		1	2	3	4	1	2	3	4	1	2	3	4	
blue	male	1	9.2	24.4	59.9	6.5	0.4	27	72.6	0	36.9	24	39.1	0
	female	2	0	88	0.1	11.9	0	100	0	0	0.1	94.3	0	5.6
orange	male	3	6.4	11.1	82.5	0	11.4	0	88.6	0	39.2	9.4	51.4	0
	female	4	9.3	20.3	0.1	70.3	7.9	0.8	6.3	85	4.1	18.7	4.6	72.6
\emptyset		62.5				68.5				63.8				

APPENDIX A

DERIVATION OF M-STEP ESTIMATES

Using the matrix calculus rules from [56], [58], \mathbf{F} is a differentiable $m \times p$ matrix function of a $n \times q$ matrix \mathbf{X} . Then, the Jacobian matrix of \mathbf{F} at \mathbf{X} is a $mp \times nq$ matrix

$$D\mathbf{F}(\mathbf{X}) = \frac{\partial \text{vec}(\mathbf{F}(\mathbf{X}))}{\partial (\text{vec}(\mathbf{X}))^\top}. \quad (45)$$

Starting with the differential of the complete data log-likelihood regarding ξ_m , we define \mathbf{F} as a 1×1 scalar function of the $r \times 1$ vector ξ_m . Hence, the resulting Jacobian matrix is just the gradient and is of size $1 \times r$. Setting \mathbf{F} equal to (34), i.e.,

$$\mathbf{F}(\xi_m) = \sum_{n=1}^N \sum_{m=1}^l v_{nm} (\ln(\gamma_m) + \ln(f_s(\mathbf{x}_n | \theta_m))) \quad (46)$$

and applying the differential leads to

$$\begin{aligned} d\mathbf{F}(\xi_m) &= \sum_{n=1}^N v_{nm} d(\ln(f_s(\mathbf{x}_n | \theta_m))) \\ &= \sum_{n=1}^N \frac{2 \left| \Omega_m^{-1} \right|^{\frac{1}{2}}}{f_s(\mathbf{x}_n | \theta_m)} [dg(t_{nm}) F(\kappa_{nm}) + g(t_{nm}) dF(\kappa_{nm})]. \end{aligned} \quad (47)$$

Both differentials are calculated separately as

$$dg(t_{nm}) = -g'(t_{nm}) 2(\mathbf{x}_n - \xi_m)^\top \Omega_m^{-1} d\xi_m$$

$$= g(t_{nm}) \psi(t_{nm}) 2 \times \left((\mathbf{x}_n - \xi_m)^\top \mathbf{S}_m^{-1} - \eta_{nm} \lambda_m^\top \mathbf{S}_m^{-1} \right) d\xi_m \quad (48)$$

with

$$g'(t_{nm}) = -\psi(t_{nm}) g(t_{nm}), \quad (49)$$

the Sherman-Morrison formula [63]

$$\left(\mathbf{A} + \mathbf{bc}^\top \right)^{-1} = \mathbf{A}^{-1} - \frac{\mathbf{A}^{-1} \mathbf{bc}^\top \mathbf{A}^{-1}}{1 + \mathbf{c}^\top \mathbf{A}^{-1} \mathbf{b}} \quad (50)$$

and

$$\begin{aligned} dF(\kappa_{nm}) &= F'(\kappa_{nm}) d \left(\frac{\eta_{nm} \sqrt{2\psi(t_{nm})}}{\tau_m} \right) \\ &= -F'(\kappa_{nm}) \left[\frac{\lambda_m^\top \mathbf{S}_m^{-1} d\xi_m}{\sqrt{1 + \lambda_m^\top \mathbf{S}_m^{-1} \lambda_m}} \sqrt{2\psi(t_{nm})} \right. \\ &\quad \left. + 2 \frac{\eta_{nm}}{\tau_m} \frac{\eta(t_{nm})}{\sqrt{2\psi(t_{nm})}} (\mathbf{x}_n - \xi_m)^\top \Omega_m^{-1} d\xi_m \right] \\ &= F(\kappa_{nm}) \Psi(\kappa_{nm}) \left[\tau_m \sqrt{2\psi(t_{nm})} \lambda_m^\top \mathbf{S}_m^{-1} \right. \\ &\quad \left. + 2 \frac{\eta_{nm}}{\tau_m} \frac{\eta(t_{nm})}{\sqrt{2\psi(t_{nm})}} (\mathbf{x}_n - \xi_m)^\top \mathbf{S}_m^{-1} \right. \\ &\quad \left. - 2 \frac{\eta_{nm}^2}{\tau_m} \frac{\eta(t_{nm})}{\sqrt{2\psi(t_{nm})}} \lambda_m^\top \mathbf{S}_m^{-1} \right] d\xi_m \end{aligned} \quad (51)$$

with

$$F'(x) = -\Psi(x)F(x). \quad (52)$$

Using the scalar values

$$e_{0,nm} = 2\psi(\underline{t}_{nm}) + 2\Psi(\kappa_{nm}) \frac{\eta_{nm}}{\tau_m} \frac{\eta(\underline{t}_{nm})}{\sqrt{2\psi(\underline{t}_{nm})}}, \quad (53)$$

$$e_{1,nm} = 2\psi(\underline{t}_{nm}) \eta_{nm} - \Psi(\kappa_{nm}) \tau_m \sqrt{2\psi(\underline{t}_{nm})} \\ + \Psi(\kappa_{nm}) 2 \frac{\eta_{nm}^2}{\tau_m} \frac{\eta(\underline{t}_{nm})}{\sqrt{2\psi(\underline{t}_{nm})}} \quad (54)$$

the differentials can be combined to the gradient as follows

$$d\mathbf{F}(\boldsymbol{\xi}_m) = \sum_{n=1}^N v_{nm} \left(e_{0,nm} (\mathbf{x}_n - \boldsymbol{\xi}_m)^\top - e_{1,nm} \boldsymbol{\lambda}_m^\top \right) \mathbf{S}_m^{-1}. \quad (55)$$

Setting Equation (55) to zero and solving for $\boldsymbol{\xi}_m$ leads to the ML estimate. As discussed in Section IV, finding an exact solution, is not feasible for general RESK distributions. Therefore, the values $e_{0,nm}$ and $e_{1,nm}$, are replaced by their approximations, i.e. $\tilde{e}_{0,nm}$, $\tilde{e}_{1,nm}$. These approximations are constants with respect to the unknown parameters $\boldsymbol{\theta}_m$. They are introduced by approximating \underline{t}_{nm} , τ_m , η_{nm} , and κ_{nm} with their corresponding estimates from the previous iteration of Algorithm 1. The resulting approximate ML estimate is the obtained by setting the approximate gradient to zero:

$$\sum_{n=1}^N v_{nm} \left(\tilde{e}_{0,nm} (\mathbf{x}_n - \boldsymbol{\xi}_m)^\top - \tilde{e}_{1,nm} \boldsymbol{\lambda}_m^\top \right) \mathbf{S}_m^{-1} \stackrel{!}{=} 0 \\ \Rightarrow \sum_{n=1}^N v_{nm} (\tilde{e}_{0,nm} (\mathbf{x}_n - \boldsymbol{\xi}_m) - \tilde{e}_{1,nm} \boldsymbol{\lambda}_m) = 0 \\ \Rightarrow \hat{\boldsymbol{\xi}}_m = \frac{\sum_{n=1}^N v_{nm} (\tilde{e}_{0,nm} \mathbf{x}_n - \tilde{e}_{1,nm} \boldsymbol{\lambda}_m)}{\sum_{n=1}^N v_{nm} \tilde{e}_{0,nm}}. \quad (56)$$

Now, \mathbf{F} is defined as a 1×1 scalar function of the $r \times 1$ vector $\boldsymbol{\lambda}_m$. Hence, the resulting Jacobian matrix is just the gradient and is of size $1 \times r$. Setting \mathbf{F} equal to (29) and applying the differential gives

$$d\mathbf{F}(\boldsymbol{\lambda}_m) = \sum_{n=1}^N v_{nm} d(\ln(f_s(\mathbf{x}_n | \boldsymbol{\theta}_m))) \\ = \sum_{n=1}^N \frac{2}{f_s(\mathbf{x}_n | \boldsymbol{\theta}_m)} \left[d \left(|\boldsymbol{\Omega}_m|^{-\frac{1}{2}} \right) g(\underline{t}_{nm}) F(\kappa_{nm}) \right. \\ \left. + |\boldsymbol{\Omega}_m|^{-\frac{1}{2}} dg(\underline{t}_{nm}) F(\kappa_{nm}) \right. \\ \left. + |\boldsymbol{\Omega}_m|^{-\frac{1}{2}} g(\underline{t}_{nm}) dF(\kappa_{nm}) \right]. \quad (57)$$

Again, the occurring differentials are calculated separately. Firstly,

$$d(|\boldsymbol{\Omega}_m|^{-\frac{1}{2}}) \\ = -\frac{1}{2} |\boldsymbol{\Omega}_m|^{-\frac{1}{2}} |\boldsymbol{\Omega}_m|^{-1} |\boldsymbol{\Omega}_m| \text{Tr} \left(\boldsymbol{\Omega}_m^{-1} d\boldsymbol{\Omega}_m \right)$$

$$= -\frac{1}{2} |\boldsymbol{\Omega}_m|^{-\frac{1}{2}} \\ \times \text{Tr} \left(\left(\mathbf{S}_m^{-1} - \frac{\mathbf{S}_m^{-1} \boldsymbol{\lambda}_m \boldsymbol{\lambda}_m^\top \mathbf{S}_m^{-1}}{1 + \boldsymbol{\lambda}_m^\top \mathbf{S}_m^{-1} \boldsymbol{\lambda}_m} \right) d \left(\boldsymbol{\lambda}_m \boldsymbol{\lambda}_m^\top \right) \right) \\ = -\frac{1}{2} |\boldsymbol{\Omega}_m|^{-\frac{1}{2}} \left[\text{vec} \left(\mathbf{S}_m^{-1} \right)^\top \right. \\ \left. - \tau_m^2 \text{vec} \left(\mathbf{S}_m^{-1} \boldsymbol{\lambda}_m \boldsymbol{\lambda}_m^\top \mathbf{S}_m^{-1} \right)^\top \right] d\text{vec} \left(\boldsymbol{\lambda}_m \boldsymbol{\lambda}_m^\top \right) \\ = -\frac{1}{2} |\boldsymbol{\Omega}_m|^{-\frac{1}{2}} \left[\text{vec} \left(\mathbf{S}_m^{-1} \boldsymbol{\lambda}_m \right)^\top + \text{vec} \left(\boldsymbol{\lambda}_m^\top \mathbf{S}_m^{-1} \right)^\top \right. \\ \left. - \tau_m^2 \left[\boldsymbol{\lambda}_m^\top \mathbf{S}_m^{-1} \boldsymbol{\lambda}_m \otimes \boldsymbol{\lambda}_m^\top \mathbf{S}_m^{-1} \right. \right. \\ \left. \left. + \boldsymbol{\lambda}_m^\top \mathbf{S}_m^{-1} \otimes \boldsymbol{\lambda}_m^\top \mathbf{S}_m^{-1} \boldsymbol{\lambda}_m \right] \right] d\boldsymbol{\lambda}_m \\ = -|\boldsymbol{\Omega}_m|^{-\frac{1}{2}} \tau_m^2 \boldsymbol{\lambda}_m^\top \mathbf{S}_m^{-1} d\boldsymbol{\lambda}_m, \quad (58)$$

with

$$d\text{vec} \left(\boldsymbol{\lambda}_m \boldsymbol{\lambda}_m^\top \right) = \left((\boldsymbol{\lambda}_m \otimes \mathbf{I}_r) + (\mathbf{I}_r \otimes \boldsymbol{\lambda}_m) \right) d\boldsymbol{\lambda}_m. \quad (59)$$

Secondly, with $\tilde{\mathbf{x}}_n = \mathbf{x}_n - \boldsymbol{\xi}_m$

$$dg(\underline{t}_{nm}) = g'(\underline{t}_{nm}) \tilde{\mathbf{x}}_n^\top d \left(\boldsymbol{\Omega}_m^{-1} \right) \tilde{\mathbf{x}}_n \\ = -g'(\underline{t}_{nm}) \tilde{\mathbf{x}}_n^\top \left(\mathbf{S}_m + \boldsymbol{\lambda}_m \boldsymbol{\lambda}_m^\top \right)^{-1} \\ \times d \left(\mathbf{S}_m + \boldsymbol{\lambda}_m \boldsymbol{\lambda}_m^\top \right) \left(\mathbf{S}_m + \boldsymbol{\lambda}_m \boldsymbol{\lambda}_m^\top \right)^{-1} \tilde{\mathbf{x}}_n \\ = -g'(\underline{t}_{nm}) \left(\tilde{\mathbf{x}}_n^\top \mathbf{S}_m^{-1} - \eta_{nm} \boldsymbol{\lambda}_m^\top \mathbf{S}_m^{-1} \right) \\ \times d \left(\boldsymbol{\lambda}_m \boldsymbol{\lambda}_m^\top \right) \left(\tilde{\mathbf{x}}_n^\top \mathbf{S}_m^{-1} - \eta_{nm} \boldsymbol{\lambda}_m^\top \mathbf{S}_m^{-1} \right) \quad (60)$$

with vectorization

$$d\text{vec} \left(g(\underline{t}_{nm}) \right) \\ = -g'(\underline{t}_{nm}) \left[\left(\tilde{\mathbf{x}}_n^\top \mathbf{S}_m^{-1} - \eta_{nm} \boldsymbol{\lambda}_m^\top \mathbf{S}_m^{-1} \right) \right. \\ \left. \otimes \left(\tilde{\mathbf{x}}_n^\top \mathbf{S}_m^{-1} - \eta_{nm} \boldsymbol{\lambda}_m^\top \mathbf{S}_m^{-1} \right) \right] d\text{vec} \left(\boldsymbol{\lambda}_m \boldsymbol{\lambda}_m^\top \right) \\ = g(\underline{t}_{nm}) \psi(\underline{t}_{nm}) 2 \left(\eta_{nm} \tilde{\mathbf{x}}_n^\top \mathbf{S}_m^{-1} - \eta_{nm}^2 \boldsymbol{\lambda}_m^\top \mathbf{S}_m^{-1} \right) d\boldsymbol{\lambda}_m \quad (61)$$

and thirdly

$$dF(\kappa_{nm}) \\ = F'(\kappa_{nm}) d \left(\frac{\boldsymbol{\lambda}_m^\top \mathbf{S}_m^{-1} \tilde{\mathbf{x}}_n}{\sqrt{1 + \boldsymbol{\lambda}_m^\top \mathbf{S}_m^{-1} \boldsymbol{\lambda}_m}} \sqrt{2\psi(\underline{t}_{nm})} \right) \\ = F'(\kappa_{nm}) \left[\tau_m \sqrt{2\psi(\underline{t}_{nm})} d \left(\boldsymbol{\lambda}_m^\top \right) \mathbf{S}_m^{-1} \tilde{\mathbf{x}}_n \right. \\ \left. - \frac{\eta_{nm}}{\tau_m} \sqrt{2\psi(\underline{t}_{nm})} \tau_m^2 \frac{d \left(1 + \boldsymbol{\lambda}_m^\top \mathbf{S}_m^{-1} \boldsymbol{\lambda}_m \right)}{2\sqrt{1 + \boldsymbol{\lambda}_m^\top \mathbf{S}_m^{-1} \boldsymbol{\lambda}_m}} \right. \\ \left. + \frac{\eta_{nm}}{\tau_m} \frac{\eta(\underline{t}_{nm})}{\sqrt{2\psi(\underline{t}_{nm})}} \tilde{\mathbf{x}}_n^\top d \left(\boldsymbol{\Omega}_m^{-1} \right) \tilde{\mathbf{x}}_n \right]$$

$$\begin{aligned}
&= F'(\kappa_{nm}) \left[\tau_m \sqrt{2\psi(\underline{t}_{nm})} \mathbf{d} \left(\boldsymbol{\lambda}_m^\top \right) \mathbf{S}_m^{-1} \tilde{\mathbf{x}}_n \right. \\
&\quad - \frac{1}{2} \eta_{nm} \tau_m \sqrt{2\psi(\underline{t}_{nm})} \mathbf{d} \left(\boldsymbol{\lambda}_m^\top \mathbf{S}_m^{-1} \boldsymbol{\lambda}_m \right) \\
&\quad - \frac{\eta_{nm}}{\tau_m} \frac{\eta(\underline{t}_{nm})}{\sqrt{2\psi(\underline{t}_{nm})}} \left(\tilde{\mathbf{x}}_n^\top \mathbf{S}_m^{-1} - \eta_{nm} \boldsymbol{\lambda}_m^\top \mathbf{S}_m^{-1} \right) \\
&\quad \left. \times \mathbf{d} \left(\boldsymbol{\lambda}_m \boldsymbol{\lambda}_m^\top \right) \left(\mathbf{S}_m^{-1} \tilde{\mathbf{x}}_n - \eta_{nm} \mathbf{S}_m^{-1} \boldsymbol{\lambda}_m \right) \right] \quad (62)
\end{aligned}$$

with vectorization

$$\begin{aligned}
&\text{dvec} \left(F(\kappa_{nm}) \right) \\
&= F'(\kappa_{nm}) \left[\tau_m \sqrt{2\psi(\underline{t}_{nm})} \left(\tilde{\mathbf{x}}_n^\top \mathbf{S}_m^{-1} \otimes \mathbf{I}_1 \right) \mathbf{d} \boldsymbol{\lambda}_m^\top \right. \\
&\quad - \frac{1}{2} \eta_{nm} \tau_m \sqrt{2\psi(\underline{t}_{nm})} \text{dvec} \left(\boldsymbol{\lambda}_m^\top \mathbf{S}_m^{-1} \boldsymbol{\lambda}_m \right) \\
&\quad - \frac{\eta_{nm}}{\tau_m} \frac{\eta(\underline{t}_{nm})}{\sqrt{2\psi(\underline{t}_{nm})}} \left(\left(\tilde{\mathbf{x}}_n^\top \mathbf{S}_m^{-1} - \eta_{nm} \boldsymbol{\lambda}_m^\top \mathbf{S}_m^{-1} \right) \right. \\
&\quad \left. \otimes \left(\tilde{\mathbf{x}}_n^\top \mathbf{S}_m^{-1} - \eta_{nm} \boldsymbol{\lambda}_m^\top \mathbf{S}_m^{-1} \right) \right) \text{dvec} \left(\boldsymbol{\lambda}_m \boldsymbol{\lambda}_m^\top \right) \left. \right] \\
&= -F(\kappa_{nm}) \Psi(\kappa_{nm}) \left[\tau_m \sqrt{2\psi(\underline{t}_{nm})} \tilde{\mathbf{x}}_n^\top \mathbf{S}_m^{-1} \right. \\
&\quad - \eta_{nm} \tau_m \sqrt{2\psi(\underline{t}_{nm})} \boldsymbol{\lambda}_m^\top \mathbf{S}_m^{-1} - \frac{\eta_{nm}}{\tau_m} \frac{2\eta(\underline{t}_{nm})}{\sqrt{2\psi(\underline{t}_{nm})}} \tilde{\mathbf{x}}_n^\top \mathbf{S}_m^{-1} \\
&\quad \left. + \frac{\eta_{nm}^3}{\tau_m} \frac{2\eta(\underline{t}_{nm})}{\sqrt{2\psi(\underline{t}_{nm})}} \boldsymbol{\lambda}_m^\top \mathbf{S}_m^{-1} \right] \mathbf{d} \boldsymbol{\lambda}_m. \quad (63)
\end{aligned}$$

Combining the differentials with

$$\begin{aligned}
e_{2,nm} &= \tau_m^2 + \psi(\underline{t}_{nm}) 2\eta_{nm}^2 - \Psi(\kappa_{nm}) \eta_{nm} \tau_m \sqrt{2\psi(\underline{t}_{nm})} \\
&\quad + \Psi(\kappa_{nm}) 2 \frac{\eta_{nm}^3}{\tau_m} \frac{\eta(\underline{t}_{nm})}{\sqrt{2\psi(\underline{t}_{nm})}} \quad (64)
\end{aligned}$$

the gradient becomes

$$\mathbf{DF}(\boldsymbol{\lambda}_m) = \sum_{n=1}^N v_{nm} \left(e_{1,nm} \tilde{\mathbf{x}}_n^\top \mathbf{S}_m^{-1} - e_{2,nm} \boldsymbol{\lambda}_m^\top \mathbf{S}_m^{-1} \right). \quad (65)$$

Analogously to Eq. (55), the gradient in Eq. (65) is approximated by replacing $e_{1,nm}$ and $e_{2,nm}$ by their approximations, i.e. $\tilde{e}_{1,nm}$, $\tilde{e}_{2,nm}$. Then, the approximate ML estimate follows by setting the approximate gradient to zero and solving for $\boldsymbol{\lambda}_m$:

$$\hat{\boldsymbol{\lambda}}_m = \frac{\sum_{n=1}^N v_{nm} \tilde{e}_{1,nm} \tilde{\mathbf{x}}_n}{\sum_{n=1}^N v_{nm} \tilde{e}_{2,nm}}. \quad (66)$$

Lastly, F is defined as a 1×1 scalar function of the $r \times r$ matrix \mathbf{S}_m . Hence, the resulting Jacobian matrix is just the gradient and is of size $1 \times r^2$. Setting F equal to (29) and applying the differential

$$\mathbf{dF}(\mathbf{S}_m) = \sum_{n=1}^N v_{nm} \mathbf{d} \left(\ln(f_s(\mathbf{x}_n | \boldsymbol{\theta}_m)) \right)$$

$$\begin{aligned}
&= \sum_{n=1}^N \frac{2}{f_s(\mathbf{x}_n | \boldsymbol{\theta}_m)} \left[\mathbf{d} \left(\left| \boldsymbol{\Omega}_m^{-1} \right|^{\frac{1}{2}} \right) g(\underline{t}_{nm}) F(\kappa_{nm}) \right. \\
&\quad + \left| \boldsymbol{\Omega}_m^{-1} \right|^{\frac{1}{2}} \mathbf{d} g(\underline{t}_{nm}) F(\kappa_{nm}) \\
&\quad \left. + \left| \boldsymbol{\Omega}_m^{-1} \right|^{\frac{1}{2}} g(\underline{t}_{nm}) \mathbf{d} F(\kappa_{nm}) \right], \quad (67)
\end{aligned}$$

again, leads to three differentials that are calculated separately. Starting with

$$\begin{aligned}
&\mathbf{d} \left(\left| \boldsymbol{\Omega}_m \right|^{-\frac{1}{2}} \right) \\
&= -\frac{1}{2} \left| \boldsymbol{\Omega}_m \right|^{-\frac{1}{2}} \left| \boldsymbol{\Omega}_m \right|^{-1} \left| \boldsymbol{\Omega}_m \right| \text{Tr} \left(\boldsymbol{\Omega}_m^{-1} \mathbf{d} \boldsymbol{\Omega}_m \right) \\
&= -\frac{1}{2} \left| \boldsymbol{\Omega}_m \right|^{-\frac{1}{2}} \text{Tr} \left[\mathbf{S}_m^{-1} \mathbf{d} \left(\mathbf{S}_m \right) \right. \\
&\quad \left. - \tau_m^2 \mathbf{S}_m^{-1} \boldsymbol{\lambda}_m \boldsymbol{\lambda}_m^\top \mathbf{S}_m^{-1} \mathbf{d} \left(\mathbf{S}_m \right) \right] \\
&= -\frac{1}{2} \left| \boldsymbol{\Omega}_m \right|^{-\frac{1}{2}} \left[\text{vec} \left(\mathbf{S}_m^{-1} \right)^\top \right. \\
&\quad \left. - \tau_m^2 \text{vec} \left(\mathbf{S}_m^{-1} \boldsymbol{\lambda}_m \boldsymbol{\lambda}_m^\top \mathbf{S}_m^{-1} \right)^\top \right] \text{dvec} \left(\mathbf{S}_m \right) \\
&= -\frac{1}{2} \left| \boldsymbol{\Omega}_m \right|^{-\frac{1}{2}} \left[\text{vec} \left(\mathbf{S}_m^{-1} \right)^\top \right. \\
&\quad \left. - \tau_m^2 \left(\boldsymbol{\lambda}_m^\top \mathbf{S}_m^{-1} \otimes \boldsymbol{\lambda}_m^\top \mathbf{S}_m^{-1} \right) \right] \mathbf{D}_r \text{dvech} \left(\mathbf{S}_m \right) \quad (68)
\end{aligned}$$

followed by

$$\begin{aligned}
&\mathbf{d} g(\underline{t}_{nm}) = g'(\underline{t}_{nm}) \tilde{\mathbf{x}}_n^\top \mathbf{d} \left(\boldsymbol{\Omega}_m^{-1} \right) \tilde{\mathbf{x}}_n \\
&= -g'(\underline{t}_{nm}) \tilde{\mathbf{x}}_n^\top \left(\mathbf{S}_m + \boldsymbol{\lambda}_m \boldsymbol{\lambda}_m^\top \right)^{-1} \\
&\quad \times \mathbf{d} \left(\mathbf{S}_m \right) \left(\mathbf{S}_m + \boldsymbol{\lambda}_m \boldsymbol{\lambda}_m^\top \right)^{-1} \tilde{\mathbf{x}}_n \\
&= -g'(\underline{t}_{nm}) \left(\tilde{\mathbf{x}}_n^\top \mathbf{S}_m^{-1} - \eta_{nm} \boldsymbol{\lambda}_m^\top \mathbf{S}_m^{-1} \right) \\
&\quad \times \mathbf{d} \left(\mathbf{S}_m \right) \left(\tilde{\mathbf{x}}_n^\top \mathbf{S}_m^{-1} - \eta_{nm} \boldsymbol{\lambda}_m^\top \mathbf{S}_m^{-1} \right) \quad (69)
\end{aligned}$$

with the vectorization

$$\begin{aligned}
&\text{dvec} \left(g(\underline{t}_{nm}) \right) \\
&= -g'(\underline{t}_{nm}) \left[\left(\tilde{\mathbf{x}}_n^\top \mathbf{S}_m^{-1} - \eta_{nm} \boldsymbol{\lambda}_m^\top \mathbf{S}_m^{-1} \right) \right. \\
&\quad \left. \otimes \left(\tilde{\mathbf{x}}_n^\top \mathbf{S}_m^{-1} - \eta_{nm} \boldsymbol{\lambda}_m^\top \mathbf{S}_m^{-1} \right) \right] \text{dvec} \left(\mathbf{S}_m \right) \\
&= g(\underline{t}_{nm}) \psi(\underline{t}_{nm}) \left[\left(\tilde{\mathbf{x}}_n^\top \mathbf{S}_m^{-1} \otimes \tilde{\mathbf{x}}_n^\top \mathbf{S}_m^{-1} \right) \right. \\
&\quad - \left(\tilde{\mathbf{x}}_n^\top \mathbf{S}_m^{-1} \otimes \eta_{nm} \boldsymbol{\lambda}_m^\top \mathbf{S}_m^{-1} \right) - \left(\eta_{nm} \boldsymbol{\lambda}_m^\top \mathbf{S}_m^{-1} \otimes \tilde{\mathbf{x}}_n^\top \mathbf{S}_m^{-1} \right) \\
&\quad \left. + \left(\eta_{nm}^2 \boldsymbol{\lambda}_m^\top \mathbf{S}_m^{-1} \otimes \boldsymbol{\lambda}_m^\top \mathbf{S}_m^{-1} \right) \right] \mathbf{D}_r \text{dvech} \left(\mathbf{S}_m \right) \quad (70)
\end{aligned}$$

and finally

$$\mathbf{dF}(\kappa_{nm}) = F'(\kappa_{nm}) \mathbf{d} \left(\frac{\boldsymbol{\lambda}_m^\top \mathbf{S}_m^{-1} (\mathbf{x}_n - \boldsymbol{\xi}_m)}{\sqrt{1 + \boldsymbol{\lambda}_m^\top \mathbf{S}_m^{-1} \boldsymbol{\lambda}_m}} \sqrt{2\psi(\underline{t}_{nm})} \right)$$

$$\begin{aligned}
&= F'(\kappa_{nm}) \left[\tau_m \sqrt{2\psi(\underline{t}_{nm})} \boldsymbol{\lambda}_m^\top \mathbf{d}(\mathbf{S}_m^{-1}) \tilde{\mathbf{x}}_n \right. \\
&\quad - \frac{\eta_{nm}}{\tau_m} \sqrt{2\psi(\underline{t}_{nm})} \tau_m^2 \frac{\boldsymbol{\lambda}_m^\top \mathbf{d}(\mathbf{S}_m^{-1}) \boldsymbol{\lambda}_m}{2\sqrt{1 + \boldsymbol{\lambda}_m^\top \mathbf{S}_m^{-1} \boldsymbol{\lambda}_m}} \\
&\quad \left. + \frac{\eta_{nm}}{\tau_m} \frac{\eta(\underline{t}_{nm})}{\sqrt{2\psi(\underline{t}_{nm})}} \tilde{\mathbf{x}}_n^\top \mathbf{d}(\boldsymbol{\Omega}_m^{-1}) \tilde{\mathbf{x}}_n \right] \\
&= F'(\kappa_{nm}) \left[-\tau_m \sqrt{2\psi(\underline{t}_{nm})} \boldsymbol{\lambda}_m^\top \mathbf{S}_m^{-1} \mathbf{d}(\mathbf{S}_m) \mathbf{S}_m^{-1} \tilde{\mathbf{x}}_n \right. \\
&\quad + \frac{1}{2} \eta_{nm} \tau_m \sqrt{2\psi(\underline{t}_{nm})} \boldsymbol{\lambda}_m^\top \mathbf{S}_m^{-1} \mathbf{d}(\mathbf{S}_m) \mathbf{S}_m^{-1} \boldsymbol{\lambda}_m \\
&\quad - \frac{\eta_{nm}}{\tau_m} \frac{\eta(\underline{t}_{nm})}{\sqrt{2\psi(\underline{t}_{nm})}} \left(\tilde{\mathbf{x}}_n^\top \mathbf{S}_m^{-1} - \eta_{nm} \boldsymbol{\lambda}_m^\top \mathbf{S}_m^{-1} \right) \\
&\quad \left. \times \mathbf{d}(\mathbf{S}_m) \left(\mathbf{S}_m^{-1} \tilde{\mathbf{x}}_n - \eta_{nm} \mathbf{S}_m^{-1} \boldsymbol{\lambda}_m \right) \right] \quad (71)
\end{aligned}$$

with vectorization

$\text{dvec}(F(\kappa_{nm}))$

$$\begin{aligned}
&= F'(\kappa_{nm}) \left[-\tau_m \sqrt{2\psi(\underline{t}_{nm})} \left(\tilde{\mathbf{x}}_n^\top \mathbf{S}_m^{-1} \otimes \boldsymbol{\lambda}_m^\top \mathbf{S}_m^{-1} \right) \right. \\
&\quad + \frac{1}{2} \eta_{nm} \tau_m \sqrt{2\psi(\underline{t}_{nm})} \left(\boldsymbol{\lambda}_m^\top \mathbf{S}_m^{-1} \otimes \boldsymbol{\lambda}_m^\top \mathbf{S}_m^{-1} \right) \\
&\quad - \frac{\eta_{nm}}{\tau_m} \frac{\eta(\underline{t}_{nm})}{\sqrt{2\psi(\underline{t}_{nm})}} \left[\left(\tilde{\mathbf{x}}_n^\top \mathbf{S}_m^{-1} \otimes \tilde{\mathbf{x}}_n^\top \mathbf{S}_m^{-1} \right) \right. \\
&\quad - \left(\tilde{\mathbf{x}}_n^\top \mathbf{S}_m^{-1} \otimes \eta_{nm} \boldsymbol{\lambda}_m^\top \mathbf{S}_m^{-1} \right) - \left(\eta_{nm} \boldsymbol{\lambda}_m^\top \mathbf{S}_m^{-1} \otimes \tilde{\mathbf{x}}_n^\top \mathbf{S}_m^{-1} \right) \\
&\quad \left. \left. + \left(\eta_{nm}^2 \boldsymbol{\lambda}_m^\top \mathbf{S}_m^{-1} \otimes \boldsymbol{\lambda}_m^\top \mathbf{S}_m^{-1} \right) \right] \right] \mathbf{D}_r \text{dvech}(\mathbf{S}_m) \\
&= F(\kappa_{nm}) \Psi(\kappa_{nm}) \left[\frac{\tau_m}{2} \sqrt{2\psi(\underline{t}_{nm})} \left(\boldsymbol{\lambda}_m^\top \mathbf{S}_m^{-1} \otimes \tilde{\mathbf{x}}_n^\top \mathbf{S}_m^{-1} \right) \right. \\
&\quad + \frac{\tau_m}{2} \sqrt{2\psi(\underline{t}_{nm})} \left(\tilde{\mathbf{x}}_n^\top \mathbf{S}_m^{-1} \otimes \boldsymbol{\lambda}_m^\top \mathbf{S}_m^{-1} \right) \\
&\quad - \frac{1}{2} \eta_{nm} \tau_m \sqrt{2\psi(\underline{t}_{nm})} \left(\boldsymbol{\lambda}_m^\top \mathbf{S}_m^{-1} \otimes \boldsymbol{\lambda}_m^\top \mathbf{S}_m^{-1} \right) \\
&\quad + \frac{\eta_{nm}}{\tau_m} \frac{\eta(\underline{t}_{nm})}{\sqrt{2\psi(\underline{t}_{nm})}} \left(\tilde{\mathbf{x}}_n^\top \mathbf{S}_m^{-1} \otimes \tilde{\mathbf{x}}_n^\top \mathbf{S}_m^{-1} \right) \\
&\quad - \frac{\eta_{nm}^2}{\tau_m} \frac{\eta(\underline{t}_{nm})}{\sqrt{2\psi(\underline{t}_{nm})}} \left(\tilde{\mathbf{x}}_n^\top \mathbf{S}_m^{-1} \otimes \boldsymbol{\lambda}_m^\top \mathbf{S}_m^{-1} \right) \\
&\quad - \frac{\eta_{nm}^2}{\tau_m} \frac{\eta(\underline{t}_{nm})}{\sqrt{2\psi(\underline{t}_{nm})}} \left(\boldsymbol{\lambda}_m^\top \mathbf{S}_m^{-1} \otimes \tilde{\mathbf{x}}_n^\top \mathbf{S}_m^{-1} \right) \\
&\quad \left. + \frac{\eta_{nm}^3}{\tau_m} \frac{\eta(\underline{t}_{nm})}{\sqrt{2\psi(\underline{t}_{nm})}} \left(\boldsymbol{\lambda}_m^\top \mathbf{S}_m^{-1} \otimes \boldsymbol{\lambda}_m^\top \mathbf{S}_m^{-1} \right) \right] \mathbf{D}_r \text{dvech}(\mathbf{S}_m). \quad (72)
\end{aligned}$$

Here, we used the following properties of the commutation and duplication matrix

$$\mathbf{K}_{n,n} = \mathbf{K}_n, \quad \mathbf{K}_n \mathbf{D}_n = \mathbf{D}_n \quad (73)$$

$$(\mathbf{A} \otimes \mathbf{b}^\top) \mathbf{K}_{n,p} = (\mathbf{b}^\top \otimes \mathbf{A}), \quad (74)$$

where $\mathbf{A} \in \mathbb{R}^{m \times n}$, $\mathbf{B} \in \mathbb{R}^{p \times q}$, $\mathbf{K}_{m,n} \in \mathbb{R}^{mn \times mn}$ and $\mathbf{b} \in \mathbb{R}^{p \times 1}$. Combining the results leads to the gradient

$$\begin{aligned}
\mathbf{DF}(\mathbf{S}_m) &= \sum_{n=1}^N v_{nm} \left[-\frac{1}{2} \text{vec}(\mathbf{S}_m^{-1})^\top \right. \\
&\quad + \frac{e_{0,nm}}{2} \left(\tilde{\mathbf{x}}_n^\top \mathbf{S}_m^{-1} \otimes \tilde{\mathbf{x}}_n^\top \mathbf{S}_m^{-1} \right) \\
&\quad - \frac{e_{1,nm}}{2} \left(\tilde{\mathbf{x}}_n^\top \mathbf{S}_m^{-1} \otimes \boldsymbol{\lambda}_m^\top \mathbf{S}_m^{-1} \right) \\
&\quad - \frac{e_{1,nm}}{2} \left(\boldsymbol{\lambda}_m^\top \mathbf{S}_m^{-1} \otimes \tilde{\mathbf{x}}_n^\top \mathbf{S}_m^{-1} \right) \\
&\quad \left. + \frac{e_{2,nm}}{2} \left(\boldsymbol{\lambda}_m^\top \mathbf{S}_m^{-1} \otimes \boldsymbol{\lambda}_m^\top \mathbf{S}_m^{-1} \right) \right] \mathbf{D}_r. \quad (75)
\end{aligned}$$

Analogously to Eq. (55) and Eq. (65), the gradient in Eq. (75) is approximated by replacing $e_{0,nm}$, $e_{1,nm}$ and $e_{2,nm}$ by their approximations, i.e. $\tilde{e}_{0,nm}$, $\tilde{e}_{1,nm}$, $\tilde{e}_{2,nm}$. Then, the approximate ML estimate follows by setting the approximate gradient to zero and solving for \mathbf{S}_m :

$$\begin{aligned}
&\sum_{n=1}^N v_{nm} \left[-\frac{1}{2} \text{vec}(\mathbf{S}_m^{-1})^\top + \frac{\tilde{e}_{0,nm}}{2} \left(\tilde{\mathbf{x}}_n^\top \mathbf{S}_m^{-1} \otimes \tilde{\mathbf{x}}_n^\top \mathbf{S}_m^{-1} \right) \right. \\
&\quad - \frac{\tilde{e}_{1,nm}}{2} \left(\tilde{\mathbf{x}}_n^\top \mathbf{S}_m^{-1} \otimes \boldsymbol{\lambda}_m^\top \mathbf{S}_m^{-1} \right) \\
&\quad - \frac{\tilde{e}_{1,nm}}{2} \left(\boldsymbol{\lambda}_m^\top \mathbf{S}_m^{-1} \otimes \tilde{\mathbf{x}}_n^\top \mathbf{S}_m^{-1} \right) \\
&\quad \left. + \frac{\tilde{e}_{2,nm}}{2} \left(\boldsymbol{\lambda}_m^\top \mathbf{S}_m^{-1} \otimes \boldsymbol{\lambda}_m^\top \mathbf{S}_m^{-1} \right) \right] \mathbf{D}_r \stackrel{!}{=} 0 \\
&\Rightarrow \sum_{n=1}^N v_{nm} \text{vec}(\mathbf{S}_m^{-1})^\top (\mathbf{S}_m \otimes \mathbf{S}_m) \\
&= \sum_{n=1}^N v_{nm} \left[\tilde{e}_{0,nm} \left(\tilde{\mathbf{x}}_n^\top \otimes \tilde{\mathbf{x}}_n^\top \right) - \tilde{e}_{1,nm} \left(\tilde{\mathbf{x}}_n^\top \otimes \boldsymbol{\lambda}_m^\top \right) \right. \\
&\quad \left. - \tilde{e}_{1,nm} \left(\boldsymbol{\lambda}_m^\top \otimes \tilde{\mathbf{x}}_n^\top \right) + \tilde{e}_{2,nm} \left(\boldsymbol{\lambda}_m^\top \otimes \boldsymbol{\lambda}_m^\top \right) \right] \\
&\Rightarrow \text{vec}(\mathbf{S}_m) = \left[\sum_{n=1}^N v_{nm} \left[\tilde{e}_{0,nm} \left(\tilde{\mathbf{x}}_n \otimes \tilde{\mathbf{x}}_n \right) \right. \right. \\
&\quad - \tilde{e}_{1,nm} \left(\tilde{\mathbf{x}}_n \otimes \boldsymbol{\lambda}_m \right) - \tilde{e}_{1,nm} \left(\boldsymbol{\lambda}_m \otimes \tilde{\mathbf{x}}_n \right) \\
&\quad \left. \left. + \tilde{e}_{2,nm} \left(\boldsymbol{\lambda}_m \otimes \boldsymbol{\lambda}_m \right) \right] \right] / \sum_{n=1}^N v_{nm} \\
&\Rightarrow \hat{\mathbf{S}}_m = \left[\sum_{n=1}^N v_{nm} \left(\tilde{e}_{0,nm} \tilde{\mathbf{x}}_n \tilde{\mathbf{x}}_n^\top - \tilde{e}_{1,nm} \tilde{\mathbf{x}}_n \boldsymbol{\lambda}_m^\top \right. \right. \\
&\quad \left. \left. - \tilde{e}_{1,nm} \boldsymbol{\lambda}_m \tilde{\mathbf{x}}_n^\top + \tilde{e}_{2,nm} \boldsymbol{\lambda}_m \boldsymbol{\lambda}_m^\top \right) \right] / \sum_{n=1}^N v_{nm}. \quad (76)
\end{aligned}$$

Finally, we have to maximize with regard to the mixing coefficients γ_m . Because they have the constraint

$$\sum_{m=1}^l \gamma_m = 1 \quad (77)$$

a Lagrange multiplier is used

$$\mathbf{dF}(\gamma_m) = \sum_{n=1}^N v_{nm} \mathbf{d}(\ln(\gamma_m)) + \lambda \mathbf{d} \left(\sum_{m=1}^l \gamma_m - 1 \right)$$

$$= \sum_{n=1}^N \frac{v_{nm}}{\gamma_m} + \lambda. \quad (78)$$

First, we solve for λ

$$\begin{aligned} 0 &\stackrel{!}{=} \sum_{n=1}^N \frac{v_{nm}}{\gamma_m} + \lambda \\ \Rightarrow -\lambda \sum_{m=1}^l \gamma_m &= \sum_{n=1}^N \sum_{m=1}^l v_{nm} \\ \Rightarrow \lambda &= -N \end{aligned} \quad (79)$$

and, after the elimination of λ , we find

$$\hat{\gamma}_m = \frac{1}{N} \sum_{n=1}^N v_{nm}. \quad (80)$$

ACKNOWLEDGMENT

Christian A. Schroth is supported by the DFG Project Number 431431951. The work of Michael Muma has been funded by the LOEWE initiative (Hesse, Germany) within the emergenCITY centre and is supported by the ‘Athene Young Investigator Programme’ of Technische Universität Darmstadt, Hesse, Germany.

REFERENCES

- [1] A. P. Dempster, N. M. Laird, and D. B. Rubin, “Maximum Likelihood from Incomplete Data via the EM Algorithm,” *Journal of the Royal Statistical Society. Series B (Methodological)*, vol. 39, no. 1, pp. 1–38, 1977.
- [2] S. Lloyd, “Least squares quantization in PCM,” *IEEE Transactions on Information Theory*, vol. 28, no. 2, pp. 129–137, 1982.
- [3] A. K. Jain and R. C. Dubes, *Algorithms for clustering data*, ser. Prentice Hall advanced reference series. Prentice-Hall, 1988.
- [4] D. Arthur and S. Vassilvitskii, “K-Means++: The Advantages of Careful Seeding,” in *Proceedings of the eighteenth annual ACM-SIAM symposium on Discrete algorithms*, H. Gabow, Ed., Society for Industrial and Applied Mathematics, 2007.
- [5] D. Xu and Y. Tian, “A Comprehensive Survey of Clustering Algorithms,” *Annals of Data Science*, vol. 2, no. 2, pp. 165–193, 2015.
- [6] A. M. Zoubir, V. Koivunen, Y. Chakhchoukh, and M. Muma, “Robust Estimation in Signal Processing: A Tutorial-Style Treatment of Fundamental Concepts,” *IEEE Signal Processing Magazine*, vol. 29, no. 4, pp. 61–80, 2012.
- [7] A. M. Zoubir, V. Koivunen, E. Ollila, and M. Muma, *Robust Statistics for Signal Processing*. Cambridge University Press, 2018, vol. 25.
- [8] B. Kadioglu, I. Yildiz, P. Closas, and D. Erdogmus, “M-Estimation-Based Subspace Learning for Brain Computer Interfaces,” *IEEE Journal of Selected Topics in Signal Processing*, vol. 12, no. 6, pp. 1276–1285, 2018.
- [9] P. J. Huber and E. M. Ronchetti, *Robust Statistics*, ser. Wiley Series in Probability and Statistics. Wiley, 2011.
- [10] E. Ollila and D. E. Tyler, “Regularized M-Estimators of Scatter Matrix,” *IEEE Transactions on Signal Processing*, vol. 62, no. 22, pp. 6059–6070, 2014.
- [11] R. A. Maronna, D. R. Martin, V. J. Yohai, and M. Salibián-Barrera, *Robust Statistics: Theory and Methods (with R)*, ser. Wiley Series in Probability and Statistics. Wiley, 2018.
- [12] J. Liu and D. P. Palomar, “Regularized robust estimation of mean and covariance matrix for incomplete data,” *Signal Processing*, vol. 165, pp. 278–291, 2019.
- [13] K. Wang, S.-K. Ng, and G. J. McLachlan, “Multivariate Skew t Mixture Models: Applications to Fluorescence-Activated Cell Sorting Data,” in *Digital Image Computing: Techniques and Applications*, H. Shi, Ed., Piscataway, NJ: IEEE, 2009, pp. 526–531.
- [14] S. Pyne, X. Hu, K. Wang, E. Rossin, T.-I. Lin, L. M. Maier, C. Baecher-Allan, G. J. McLachlan, P. Tamayo, D. A. Hafler, P. L. de Jager, and J. P. Mesirov, “Automated high-dimensional flow cytometric data analysis,” *Proceedings of the National Academy of Sciences of the United States of America*, vol. 106, no. 21, pp. 8519–8524, 2009.
- [15] P. Ciosas and J. Vila-Valls, “NLOS mitigation in TOA-based indoor localization by nonlinear filtering under skew t-distributed measurement noise,” in *2016 IEEE Statistical Signal Processing Workshop (SSP)*, IEEE, 2016, pp. 1–5.
- [16] W. Youn, Y. Huang, and H. Myung, “Robust Localization Using IMM Filter Based on Skew Gaussian-Gamma Mixture Distribution in Mixed LOS/NLOS Condition,” *IEEE Transactions on Instrumentation and Measurement*, pp. 1–17, 2019.
- [17] M. Bernardi, A. Maruotti, and L. Petrella, “Skew mixture models for loss distributions: A Bayesian approach,” *Insurance: Mathematics and Economics*, vol. 51, no. 3, pp. 617–623, 2012.
- [18] C. M. Bishop, *Pattern Recognition and Machine Learning*, ser. Information science and statistics. New York, NY: Springer, 2009.
- [19] M. Wang, Z. B. Abrams, S. M. Kornblau, and K. R. Coombes, “Thresher: determining the number of clusters while removing outliers,” *BMC Bioinformatics*, vol. 19, 2018.
- [20] N. Neykov, P. Filzmoser, R. Dimova, and P. Neytchev, “Robust fitting of mixtures using the trimmed likelihood estimator,” *Computational Statistics & Data Analysis*, vol. 52, no. 1, pp. 299–308, 2007.
- [21] M. T. Gallegos and G. Ritter, “Trimming algorithms for clustering contaminated grouped data and their robustness,” *Advances in Data Analysis and Classification*, vol. 3, no. 2, pp. 135–167, 2009.
- [22] —, “Using combinatorial optimization in model-based trimmed clustering with cardinality constraints,” *Computational Statistics & Data Analysis*, vol. 54, no. 3, pp. 637–654, 2010.
- [23] F. Greselin and S. Ingrassia, “Constrained monotone EM algorithms for mixtures of multivariate t distributions,” *Statistics and Computing*, vol. 20, no. 1, pp. 9–22, 2010.
- [24] J. L. Andrews and P. D. McNicholas, “Model-based clustering, classification, and discriminant analysis via mixtures of multivariate t-distributions,” *Statistics and Computing*, vol. 22, no. 5, pp. 1021–1029, 2012.
- [25] P. D. McNicholas and S. Subedi, “Clustering gene expression time course data using mixtures of multivariate t-distributions,” *Journal of Statistical Planning and Inference*, vol. 142, no. 5, pp. 1114–1127, 2012.
- [26] C. Fraley, “How Many Clusters? Which Clustering Method? Answers Via Model-Based Cluster Analysis,” *The Computer Journal*, vol. 41, no. 8, pp. 578–588, 1998.
- [27] A. Dasgupta and A. E. Raftery, “Detecting Features in Spatial Point Processes with Clutter via Model-Based Clustering,” *Journal of the American Statistical Association*, vol. 93, no. 441, p. 294, 1998.
- [28] A. Punzo and P. D. McNicholas, *Parsimonious mixtures of multivariate contaminated normal distributions*, 2013. [Online]. Available: <http://arxiv.org/pdf/1305.4669v5>.
- [29] V. Roizman, M. Jonckheere, and F. Pascal, *A flexible EM-like clustering algorithm for noisy data*, 2019. [Online]. Available: <http://arxiv.org/pdf/1907.01660v2>.
- [30] C. A. Schroth and M. Muma, “Robust M-Estimation Based Bayesian Cluster Enumeration for Real Elliptically Symmetric Distributions,” *IEEE Transactions on Signal Processing (Early Access)*, 2021.
- [31] A. Azzalini and A. Dalla Valle, “The multivariate skew-normal distribution,” *Biometrika*, vol. 83, no. 4, pp. 715–726, 1996.
- [32] A. Azzalini, “The Skew-normal Distribution and Related Multivariate Families,” *Scandinavian Journal of Statistics*, vol. 32, no. 2, pp. 159–188, 2005.
- [33] A. Azzalini and A. Capitanio, “Distributions generated by perturbation of symmetry with emphasis on a multivariate skew t-distribution,” *Journal of the Royal Statistical Society: Series B (Statistical Methodology)*, vol. 65, no. 2, pp. 367–389, 2003.
- [34] S. Kotz, T. J. Kozubowski, and K. Podgórski, “Asymmetric Multivariate Laplace Distribution,” in *The Laplace Distribution and Generalizations*, S. Kotz, T. J. Kozubowski, and K. Podgórski, Eds., Boston, MA: Birkhäuser Boston, 2001, pp. 239–272.
- [35] M. G. Genton, *Skew-elliptical distributions and their applications: A journey beyond normality*. Boca Raton, Fla: Chapman & Hall/CRC, 2004. [Online]. Available: <http://search.ebscohost.com/login.aspx?direct=true&scope=site&db=nlebk&db=nlabk&AN=111128>.
- [36] A. Azzalini and A. Capitanio, *The Skew-Normal and Related Families*. Cambridge: Cambridge University Press, 2013.

- [37] S. X. Lee and G. J. McLachlan, "On mixtures of skew normal and skew t -distributions," *Advances in Data Analysis and Classification*, vol. 7, no. 3, pp. 241–266, 2013.
- [38] A. Azzalini, R. P. Browne, M. G. Genton, and P. D. McNicholas, *On nomenclature for, and the relative merits of, two formulations of skew distributions*, 2014. [Online]. Available: <http://arxiv.org/pdf/1402.5431v3>.
- [39] R. B. Arellano-Valle, H. Bolfarine, and V. H. Lachos, "Skew-normal Linear Mixed Models," *Journal of Data Science*, pp. 415–438, 2005. [Online]. Available: <https://pdfs.semanticscholar.org/1b74/ef01b36c4f7cdc3c2255c5fdc989a2f5197b.pdf>.
- [40] M. D. Branco and D. K. Dey, "A General Class of Multivariate Skew-Elliptical Distributions," *Journal of Multivariate Analysis*, vol. 79, no. 1, pp. 99–113, 2001.
- [41] S. K. Sahu, D. K. Dey, and M. D. Branco, "A new Class of Multivariate Skew Distributions with Applications to Bayesian Regression Models," *Canadian Journal of Statistics*, vol. 31, no. 2, pp. 129–150, 2003.
- [42] T.-I. Lin, "Maximum likelihood estimation for multivariate skew normal mixture models," *Journal of Multivariate Analysis*, vol. 100, no. 2, pp. 257–265, 2009.
- [43] I. Vrbik and P. D. McNicholas, "Analytic calculations for the EM algorithm for multivariate skew-mixture models," *Statistics & Probability Letters*, vol. 82, no. 6, pp. 1169–1174, 2012.
- [44] C. R. B. Cabral, V. H. Lachos, and M. O. Prates, "Multivariate mixture modeling using skew-normal independent distributions," *Computational Statistics & Data Analysis*, vol. 56, no. 1, pp. 126–142, 2012.
- [45] I. Vrbik and P. D. McNicholas, "Parsimonious skew mixture models for model-based clustering and classification," *Computational Statistics & Data Analysis*, vol. 71, pp. 196–210, 2014.
- [46] I. Vrbik, "Non-Elliptical and Fractionally-Supervised Classification," Ph.D. dissertation, The University of Guelph, Guelph, Ontario, Canada, 2014. [Online]. Available: https://atrium.lib.uoguelph.ca/xmlui/bitstream/handle/10214/8096/Vrbik_Irene_201405_PhD.pdf?sequence=1&isAllowed=y.
- [47] S. Pyne, X. Hu, K. Wang, E. Rossin, T.-I. Lin, L. M. Maier, C. Baecher-Allan, G. J. McLachlan, P. Tamayo, D. A. Hafler, P. L. de Jager, and J. P. Mesirov, "Supplementary Information: Automated high-dimensional flow cytometric data analysis," *Proceedings of the National Academy of Sciences of the United States of America*, vol. 106, no. 21, pp. 8519–8524, 2009.
- [48] T.-I. Lin, "Robust mixture modeling using multivariate skew t distributions," *Statistics and Computing*, vol. 20, no. 3, pp. 343–356, 2010.
- [49] S. X. Lee and G. J. McLachlan, "Finite mixtures of multivariate skew t -distributions: some recent and new results," *Statistics and Computing*, vol. 24, no. 2, pp. 181–202, 2014.
- [50] U. J. Dang, M. P. B. Gallagher, R. P. Browne, and P. D. McNicholas, *Model-based clustering and classification using mixtures of multivariate skewed power exponential distributions*, 2019. [Online]. Available: <http://arxiv.org/pdf/1907.01938v1>.
- [51] R. P. Browne and P. D. McNicholas, "A mixture of generalized hyperbolic distributions," *Canadian Journal of Statistics*, vol. 43, no. 2, pp. 176–198, 2015.
- [52] G. Schwarz, "Estimating the Dimension of a Model," *The Annals of Statistics*, vol. 6, no. 2, pp. 461–464, 1978.
- [53] J. Cavanaugh and A. Neath, "Generalizing the derivation of the schwarz information criterion," *Communications in Statistics - Theory and Methods*, vol. 28, no. 1, pp. 49–66, 1999.
- [54] P. M. Djurić, "Asymptotic MAP criteria for model selection," *IEEE Transactions on Signal Processing*, vol. 46, no. 10, pp. 2726–2735, 1998.
- [55] P. Stoica and Y. Selen, "Model-Order Selection," *IEEE Signal Processing Magazine*, vol. 21, no. 4, pp. 36–47, 2004.
- [56] J. R. Magnus and H. Neudecker, *Matrix differential calculus with applications in statistics and econometrics*, ser. Wiley Series in Probability and Statistics. Wiley, 2007.
- [57] E. Ollila, I. Solovychik, D. E. Tyler, and A. Wiesel, *Simultaneous penalized M -estimation of covariance matrices using geodesically convex optimization*, 2016. [Online]. Available: <http://arxiv.org/pdf/1608.08126v1>.
- [58] K. M. Abadir and J. R. Magnus, *Matrix Algebra*, ser. Econometric Exercises. Cambridge University Press, 2005, vol. 1.
- [59] F. K. Teklehaymanot, M. Muma, and A. M. Zoubir, "Bayesian Cluster Enumeration Criterion for Unsupervised Learning," *IEEE Transactions on Signal Processing*, vol. 66, no. 20, pp. 5392–5406, 2018.
- [60] ———, "Robust Bayesian cluster enumeration based on the t distribution," *Signal Processing*, vol. 182, p. 107870, 2020.
- [61] D. J. C. MacKay, *Information Theory, Inference, and Learning Algorithms*. Cambridge University Press, 2011.
- [62] N. A. Campbell and R. J. Mahon, "A multivariate study of variation in two species of rock crab of the genus *Leptograpsus*," *Australian Journal of Zoology*, vol. 22, no. 3, p. 417, 1974.
- [63] M. S. Bartlett, "An Inverse Matrix Adjustment Arising in Discriminant Analysis," *The Annals of Mathematical Statistics*, vol. 22, no. 1, pp. 107–111, 1951.